M.Tech(PowerElectronicsandSystems)

Govind Singh

2026

Controller Design for a Boost Converter using Constrained Stability Boundary Locus

A DISSERTATION

SUBMITTED IN PARTIAL FULFILLMENT OF THE REQUIREMENTS

FOR THE AWARD OF THE DEGREE

OF

MASTER OF TECHNOLOGY

IN

POWER ELECTRONICS AND SYSTEMS

Submitted by:

GOVIND SINGH

2K24/PES/05

Under the supervision of

Dr.Ram ji Lal Meena

(Associate Professor, EED, DTU)

Mr. Gaurav Kaushik

(Assistant Professor, EED, DTU)

DEPARTMENT OF ELECTRICAL ENGINEERING

DELHI TECHNOLOGICAL UNIVERSITY

(Formerly Delhi College of Engineering)

Bawana Road, Delhi-110042

MAY, 2026

DEPARTMENT OF ELECTRICAL ENGINEERING

DELHI TECHNOLOGICAL UNIVERSITY

(Formerly Delhi College of Engineering) Bawana Road, Delhi-110042

CANDIDATE'S DECLARATION

I, **Govind Singh**, Roll No. 2K24/PES/05 student of M.Tech (Power Electronics & Systems), hereby declare that the project Dissertation titled "**Controller Design for Boost converter using Constrained Stability Boundary Locus**" which is submitted by me to the Department of Electrical Engineering, Delhi Technological university, Delhi in partial fulfilment of the requirement for the award of the degree of Master of Technology, is original and not copied from any source without proper citation. This work has not previously formed the basis for the award of any Degree, Diploma Associateship, Fellowship, or other similar title or recognition.

Place: Delhi **(Govind Singh)**

Date: 31th May 2026

DEPARTMENT OF ELECTRICAL ENGINEERING

DELHI TECHNOLOGICAL UNIVERSITY

(Formerly Delhi College of Engineering) Bawana Road, Delhi-110042

CERTIFICATE

We hereby certify that the project Dissertation titled **"Controller design for Boost Converter using Constrained Stability Boundary Locus"** which is Submitted by Govind Singh, Roll No. 2K24/PES/05, Department of Electrical Engineering, Delhi Technological University, Delhi in partial fulfilment of the requirement for the award of the degree of Master of Technology, is a record of the project work carried out by the student under my supervision. To the best of my knowledge, this work has not been submitted in part or full for any Degree or Diploma to this University or elsewhere.

Dr.Ram ji Lal Meena
Associate Professor
Department of Electrical Engineering
Delhi Technological University, Delhi

Mr. Gaurav Kaushik
Assistant Professor
Department of Electrical Engineering
Delhi Technological University, Delhi

Place: Delhi

Date: 31st May 2026

DEPARTMENT OF ELECTRICAL ENGINEERING

DELHI TECHNOLOGICAL UNIVERSITY

(Formerly Delhi College of Engineering) Bawana Road, Delhi-110042

ACKNOWLEDGEMENT

I would like to express my heartfelt gratitude to all those who contributed their valuable time, guidance, and support to help me throughout this project. Without their assistance, it would not have been possible for me to understand and successfully complete this work. First and foremost, I would like to extend my sincere thanks to **Dr. Ram ji Lal Meena** and **Mr. Gaurav Kaushik**, Associate Professors, **Department of Electrical Engineering**, Delhi Technology University for their constant support, motivation, and encouragement throughout the duration of the project. Their insightful guidance, constructive feedback and willingness to help at every stage were instrumental in the completion of this work.

Finally, I want to express my sincere gratitude to my parents, elders, and friends for their constant encouragement and support, which gave me the will and confidence to continue this research.

Date: 31st May 2026

GOVIND SINGH

M.Tech (Power Electronics & Systems)

Roll No. 2K24/PES/05

ABSTRACT

Due to rising demands for clean energy, transition from conventional sources to renewable sources of energy is also rising. The integration of the renewable energy sources to high voltage dc bus has necessitated the use of DC DC boost converters. The intermittency of these sources can be countered effectively by the closed-loop operation of the converters. The design of the controller is critical as it provides converter with good dynamic response, and effective voltage regulation against source and load disturbances. This article aims to provide a simple, analytical, and graphical way to tune the PI/PID type controllers. The controller parameterization is done on the basis of obtained stability boundary locus which is further constrained by the boundaries obtained for gain margin, and phase margin providing the controller sufficient robustness to uncertainties. The analytical study is supported with the MATLAB simulations. A 24/110 V, 100 W boost converter has been designed and simulation results are also provided.

Keywords –*DC-DC boost converter, renewable energy integration, closed - loop control, PI controller, PID controller, stability boundary locus, voltage regulation, dynamic response, robustness analysis, MATLAB simulation, high voltage DC bus, source and load disturbances, controller tuning.*

Table of Contents

LIST OF FIGURES

LIST OF TABLE

LIST OF ABBREVATIONS

Abbreviations	Full Form
KVL	Kirchhoff's Voltage Law
KCL	Kirchhoff's Current Law
CCM	Continuous Conduction Mode
SBL	Stability Boundary Locus
RSBL	Relative Stability Boundary Locus

LIST OF SYMBOLS

Symbols	Definition
Ω	Ohm
V	Voltage
s	Second
i_L	Inductor Current
η	Efficiency
R	Resistance
f	Frequency
ω	Angular Frequency

CHAPTER 1

INTRODUCTION

1.1 General Introduction

As the demand for electrical energy continues to rise and the concerns for environmental impacts of fossil-fuel based power generation intensify, the global shift towards renewable energy systems is gaining momentum. Solar photovoltaic (PV) and wind energy are among the renewable energy sources becoming significant alternatives due to their clean, sustainable, and environmental friendly nature [1]. The electricity output of these renewable energy sources is however very low and variable, depending on changes in the environment. Accordingly, the effective power electronic converter is needed to control and improve the voltage level for its use in today's DC distribution system and industries.

The DC–DC boost converter is widely used among various power electronic converters because it can output to a higher regulated voltage with high efficiency and easy circuit configuration with low input voltage [2].

In renewable energy systems, boost converters are frequently utilised, electric vehicles, fuel-cell systems, battery-operated devices and DC microgrids. Although these benefits are provided, the dynamic performance of a boost converter is significantly influenced by fluctuations in the source voltage, switching operation and load perturbations. If the converter is not properly controlled, these factors can cause instability, overshoot, slow transient response and large steady state errors. Closed loop control methods are often used to achieve stable and efficient operation of DC–DC boost converter. The most common controllers used in industrial applications are the Proportional–Integral (PI) controller and the Proportional–Integral–Derivative (PID) controller because of its affordability, ease of use, simplicity, and good control performance [3]. Better voltage regulation, reduced steady-state error, and improved transient responsiveness under various operating circumstances are all provided by these controllers. However, the converter's overall efficiency is mainly dependent the correct choice of proportional gain, integral gain and derivative gain of the controller. In the literature, several tuning methods for PI and PID controllers have been reported, such as the Ziegler–Nichols method, frequency response techniques, optimization methods and intelligent control [4]. While these methods work well, many of them require

someone to do iterative calculations, trial and error or complex optimizations. Moreover, traditional tuning methods usually only yield a fixed gain set for the controllers; the corresponding stable operating region of the system is not clearly identified. These drawbacks have been addressed by the development of a method called the Stability Boundary Locus (SBL) method for determining stabilizing controller parameters [5]. The SBL technique is based on the frequency-domain analysis of the closed-loop characteristic equation. As a result of replacing the condition on the imaginary axis: $s=j\omega$ The characteristic equations are split into real and imaginary equations and analytic relationships between controller parameters are derived. These relationships form a stability boundary curve in the parameter plane of the controller (e.g., the Kp-Ki plane for a PI controller or the Kp-Kd plane for a PID controller) when the frequency is swept across a range of frequencies. This curve bounds the region of all possible gain combinations that allow the closed loop to be stable. The SBL method does not require repeated simulations or parameter sweeping as is the common approach. Instead, it gives a full graphical depiction of which regions of the controller gains are stable and unstable, thus giving the designer freedom to choose the gains of the controller for a given set of stability and performance requirements [5]. Further, the approach can include relative stability requirements (e.g., gain margin and phase margin) to enhance system robustness to uncertainty and disturbances. Because of these benefits, the stability boundary locus approach has received much interest for applications such as power converter systems, motor drive systems, and renewable energy systems.

A systematic design and analysis of the PI/PID controllers for a DC-DC boost converter is presented in this thesis by employing the Stability Boundary Locus method. The operating regions of the converter system are obtained analytically by determining the controller parameters to achieve the robustness and stability. For analysis and simulation, a 24 V/110 V, 100 W boost converter is considered. The suggested control approach is deployed and tested in MATLAB/Simulink to evaluate the dynamic performance of the converter under different operating conditions. The effectiveness of the designed controller is analysed in terms of voltage regulation, transient response, steady-state performance, and closed-loop stability. Extensive research has been carried out over the past several decades on the tuning and design of PI and PID controllers because these controllers are widely used in industrial control systems due to their simplicity and effectiveness [6]. Despite the development of many advanced control algorithms, PI and PID controllers continue to

dominate industrial applications because they are easy to implement, economical, and capable of providing satisfactory performance for a wide range of systems. However, determining controller gains that guarantee closed-loop stability and desired dynamic response remains a major challenge, particularly for unstable and higher-order systems.
Earlier controller design techniques mainly focused on obtaining a single set of controller parameters using empirical tuning rules or optimization procedures. Although these methods are useful for practical implementation, they do not provide complete information about the entire range of stabilizing controller gains. In many practical systems, especially in power electronic converters and industrial processes, the controller must maintain stability even under parameter uncertainties and varying operating conditions. Therefore, identifying the complete stabilizing region in the controller parameter space has become an important requirement in modern control design [8].

Several analytical methods have been proposed for calculating stabilizing PI and PID controllers. Approaches based on the Hermite-Biehler theorem and linear programming techniques have shown that stabilizing controller parameters can be obtained systematically for stable and unstable plants [9], [10]. These methods also demonstrated that the stability region may exhibit different geometrical properties depending on the characteristics of the system. However, many of these approaches involve high computational complexity and require repeated parameter sweeping to identify stable operating regions. As the order of the system increases, the computational burden of these methods also increases significantly [10].Graphical and frequency domain approaches to controller design have been added to reduce the amount of computation. The methods presented in this paper, namely those based on the Nyquist plots and singular frequency concepts, allow for a faster computation of stabilizing regions, and do not require complicated optimization procedures [11]. Even so, many graphical methods require frequency gridding over a broad operating range, potentially lengthening the calculation time, and slowing down the design efficiency of the complex system. A more direct and efficient solution to these problems is given by the Stability Boundary Locus (SBL) method. In this approach, the closed loop characteristic equation is examined after replacing s with jω in mathematical expressions are obtained by solving the equation and the real and imaginary components of the characteristic equation that relate the controller

parameters. These equations produce a curve in the controller parameter plane as the frequency is swept continuously. This curve separates the plane to stable and unstable zones for the designer to determine all the possible stabilizing gains of the controller [15].One of the key aspects of the SBL technique is its ability to facilitate relative stability analysis. While stability is an essential condition, in practical control systems, the system must also be stable with good performance namely fast settling time, minimum overshoot, good damping characteristics are also required. The closed-loop poles can be moved to a desirable location in the left-half plane to stabilise the closed-loop system. The SBL approach can be used to compute stabilizing controller gains without performing a complicated mathematical optimization while meeting the following relative stability conditions [15].The other significant benefit of the suggested scheme is that gain margin and phase margin requirements can be easily included in the controller design process. Gain margin and phase margin are important indicators of robustness and stability in practical systems. These constraints can be taken into account, and therefore, the controller can achieve good performance even if disturbances, parameter variations, and modelling uncertainties exist [9]. It is very useful in the field of renewable energy power electronic systems, where operating conditions vary continuously. This method can also be used in the design of PID controllers. There are several controller parameter planes (Kp, Ki), (Kp, Kd) and (Ki, Kd) which yield stability regions. These graphical areas give a better understanding of the relationship between the system stability and the controller's parameters. Furthermore, it has been demonstrated that the region of stability is not necessarily convex for complex systems and flexible systems [15]. Hence, graphical stability analysis becomes very critical in the selection of the desired controller gains. For this reason, the Stability Boundary Locus method is used in the modern world of power electronic applications as an attractive method to design controllers, due to its simplicity, efficiency in computation, and graphical interpretation. This method works especially well for DC-DC boost converters integrated into renewable energy systems, where reliable performance and quick dynamic response are vital to meet fluctuating source and load conditions.

1.2 Motivation of the Work

In the realm of electrical power systems, the rise in the adoption of renewable energy sources is gaining momentum, driven by the demand for sustainable and clean energy generation. Renewable energy systems like solar PV, fuel cells and wind energy are typically characterized by low output voltage and voltage fluctuations due to environmental changes and varying conditions. Thus, power conversion and voltage regulation is an important consideration for reliable and stable operation of these energies [15].Among different power electronic converters, the DC-DC boost converter is extensively used in renewable energy applications due to its capability to increase the input voltage to the required output level with high efficiency and simple circuit configuration [16]. But the nonlinear and nonlinear sensitivity of the boost converter's dynamic behavior is very sensitive to the changes in load, parameter and switching conditions. These properties can make the design of the controller more complicated, especially when achieving both fast response time and stable performance are desired [17].

The traditional method of tuning a PI and PID controller is by empirical rules, trial and error or frequency response methods. These methods are easy to use, but they do not always detect all stabilizing controller parameters. Many times it takes many tuning iterations and intensive simulation testing to get to a satisfactory performance. Besides, these methods might not ensure robustness function when different operating conditions are applied, particularly in converter applications. In recent years, a lot of research has been devoted to making up for these shortcomings with stability-based controller design approaches. The most popular approach for determining all possible stabilizing gains in a systematic fashion is known as the Stability Boundary Locus (SBL) method. The approach determines the stability-instability regions of the controller parameter plane using frequency domain analysis. Additionally, Relative stability requirements, such as gain margin and phase margin, may also be incorporated into the controller design process. [19]. The graphical representation, provided by the SBL method, provides better understanding of the dynamics of the behaviour of the controller and the system compared

to traditional tuning techniques. Using the gains in the stable operating region, good transients, better robustness and stability of the closed loop can be obtained. Moreover, the SBL approach also has the advantage of lower calculation complexity and the less repetitive tuning required in the controller design process [20].

1.3 Problem Statement

The performance of a DC-DC boost converter is significantly impacted by switching conditions, input voltage volatility, and load disturbance. In real-world renewable energy systems, these fluctuations can negatively affect the converter's dynamic characteristics and could cause overshoot, sluggish transient response, larger steady state error and instability, depending on the controller's parameters [20]. Typical controller tuning methods are usually heuristic and/or simplified design assumptions, which do not generally lead to a thorough understanding of the entire stability region of the system and might not guarantee robust performance under varying operating conditions [21]. In order to overcome these shortcomings, the goal of this thesis was to use the SBL method to build the PI/PID controllers for a DC-DC boost converter. The goal is to find the gain regions of the controller that make the system stable, and enhance the transient and steady state behavior. The proposed method allows for systematic calculations of the controller parameters, and offers increased robustness with respect to parameter uncertainties and variations in operating conditions [22].

1.4 Objectives of the Thesis

Some of the primary objectives of the thesis are listed below.

1. To simulate the DC-DC boost converter system for closed loop analysis**.**
2. To be able to design a PI/PID controller for the boost converter using Stability Boundary Locus method

3. To identify the stable operating region in the space of controller parameters.
4. To study the effect of gain margin and phase margin on the stability of a system.
5. To contrast the closed loop system's stability characteristics.
6. To simulate the designed controller using MATLAB/Simulink and validate it.
7. To examine the performance of the converter in the transient response, voltage regulation and stability.

1.5 Scope of the Thesis

In this research, the Stability Boundary Locus (SBL) technique has been used to analyze the stability behaviour and design a controller for a DC–DC boost converter. This study is focused on identifying an adequate set of parameters for the PI/PID controller that provide stable conversion of the converter with various operating conditions. Stability regions are determined and graphically shown in the controller gain plane, which gives a good insight into the acceptable range of controller parameters. Also, The robustness of the control system is investigated by looking at relative stability features like gain margin and phase margin. The effectiveness of the proposed controller design is confirmed by simulation analysis in MATLAB/Simulink.

1.6 Thesis Organization

To put the research on display in a way that is both clear and well-structured, the thesis is laid out in five chapters. You will find in Chapter 1 a general overview of DC to DC boost converters and why they are so vital to power electronics and renewable energy applications. This opening chapter also makes the case for the present study by setting out its motivation, scope and objectives, as well as defining the problem at hand. The need for sound stability analysis and controller design in order to get reliable performance from a converter is made plain here too. Chapter 2 gets into how the DC to DC boost converter works, covering its modes of operation. We construct a mathematical model of the converter using analytical methods, from which we extract the transfer function, while also looking at the dynamic characteristics one needs for any stability or controller work. Then in Chapter 3 we turn to the theory behind the (SBL) method for finding the stabilizing regions of PI/PID controllers. The process for arriving at the right controller parameters is set out in some detail. There is also a discussion of robustness, gain and phase margins and relative stability to be sure the system can hold up under changing

conditions. The final chapter, Chapter 4, is where the proposed design methodology is put to the test in MATLAB/Simulink. We have run simulations to see how the boost converter performs in various scenarios and put the results before you in the form of graphs and a comparative analysis to prove the approach is effective. of the designed controllers. Chapter 5 summarizes the major contributions and findings of the designed controllers. In this chapter, the important contributions and results of the research are detailed. An overall assessment of the proposed controller design is presented, considering its positive and negative aspects. Some ideas are given for possible enhancements and future research paths about the stability of converters and the cutting-edge control methodologies.

1.7 Literature Review

The growing dependence on renewable sources of energy and modern electronic gadgets has increased the requirement for an efficient method of energy conversion. The different sources such as solar power and fuel cell sources supply voltages that keep fluctuating from one time period to another time period. The same is true for the storage batteries. Thus there is a need for the DC to DC converters to boost and regulate the voltages. The boost converter is a relatively smaller device with lightweight, thus it can be used in electric vehicles, DC micro grid and personal devices like laptop computers. Even if boost converters are good, DC to DC boost converters are also a nonlinear time variant system owing to their high frequency switches. This is because fluctuations in the load, voltage source, and duty cycles greatly influence the operation of boost converters, thereby highlighting the importance of a controller to stabilize and control boost converters. From all control techniques, two most frequently used control methods are PI and PID. Although proportional integral controllers work well for reducing steady state errors, and the The system's dynamic performance and stability are improved using proportional integral-derivative controllers. traditional control methods only offer approximate tuning, which may not be enough for describing the behavior of highly nonlinear boost converters.

Different modelling techniques of boost converters have been proposed based on State Space averaging and small-signal analysis that result in transfer functions explaining the dynamics of converters under certain operating points. The effect of mathematical modeling of boost converters in controller design and stability analysis is critical due to

converters' behavior under certain operating conditions should be predictable [26]. In addition, some researches also suggest that the existence of right half plane zero in converters' dynamics is one of the reasons why controller design is complicated and the transient response behavior cannot be optimized [27]. Many techniques have been used to optimize the operation of converters and many intelligent control approaches were used such as fuzzy logic control, neural network, genetic algorithm, and swarm optimisation as means of controlling converter designs [28]. Such methods typically provide better robustness and dynamics compared to traditional tuning methods. Nonetheless, due to higher implementation complexity, greater computational burden and additional costs involved in employing such methods in real hardware applications, their use in several industrial settings may be limited. Because of such limitations, other tuning approaches, which involve analytical techniques, remain very popular.

One of these approaches is the (SBL) tuning method. This tuning method provides an algorithmic way of determining all possible stable regions of controller parameters on the gain plane. SBL tuning determines stability constraints by utilising the closed loop system's characteristic equations across a range of frequencies. [29]. Whereas classical tuning methods only provide single solutions, the SBL method provides a range of all possible PI/PID controller parameter values that guarantee system stability. Several researchers have successfully implemented the SBL tuning method to design controllers for various industrial control and power electronic systems [30].

Graphical representation of the stability regions allows the selection of appropriate controller gains considering the required parameters such as overshoot, settling time, gain margin, and phase margin for the system performance. Recently, remarkable success has been accomplished by applying the SBL technique in designing PI/PID controllers for DC-DC boost converters. According to the research, the choice of controllers in stable regions leads to an enhancement in transient behavior, reducing oscillations, it has been revealed that the transient behavior of the controllers gets improved, the oscillations get reduced, and the disturbance rejection capacity improves when the controllers are chosen from the stable regions [31]. Additionally, relative stability analysis related to gain margin and phase margin has been introduced in order to obtain more robust performance of the converter [32].

The performance of the controller can be validated using the simulation software like MATLAB/Simulink. Many studies reveal that a properly designed PI/PID controller improves the performance of the system considerably and makes it more stable under abrupt change in load and source conditions [33]. Comparative analysis also reveals that the SBL-based tuning technique is more robust than the classical tuning approach [34]. Even with the emergence of several techniques that can be used to control modern systems, PI and PID controllers are preferred for use in industrial processes because of their affordability and simplicity. However, selecting the stabilizing controller gains that will ensure stable operations is still a challenge that requires more investigations. In this regard, the present study is concerned with the analysis of stability and design of PI and PID controllers for a DC to DC boost converter using SBL technique. Relative stability analysis and simulations have been performed to validate the results obtained**.**

1.8 Research Gap

The majority of previous research works that investigate DC-DC boost converters employ traditional PI/PID control designs where the whole stabilisation region of the controller parameters remains unspecified. Small robustness against variations in the system's load and/or input voltage values is typically ensured by these tuning techniques. How to use the SBL technique in designing the boost converter control scheme is relatively rare and limited. Specifically, its use to find out the stabilising gains of the PI/PID controllers as well as evaluate the relative stability of the controlled system has been poorly studied. Moreover, the comparison between the stability and dynamics of the PI and PID control systems has not been investigated sufficiently yet.

CHAPTER -2

Mathematical Modelling of DC- DC Boost Converter

2.1 Introduction

The growing usage of renewable energy systems, batteries, and electric vehicles has made the need for power conversion efficient. The input voltage in many cases is not adequate for the particular requirement and needs to be boosted. Among the DC to DC converters available in practice, the boost converter is considered more popular since it offers high output voltage from a low input voltage with relatively easy circuitry and efficiency. The DC to DC boost converter is widely used in solar photovoltaic systems, fuel cell systems, uninterrupted power supply systems, and portable electronic equipment. But, the efficiency and performance of this system depend on various factors like input voltage variation, switch status, and loads. It is important to investigate these dynamic characteristics and control the process efficiently. For this reason, mathematical modelling of the converter comes into play. Mathematical modelling is very useful in mathematically describing the behavior of the converter. The mathematical model describes the interaction of several important variables like inductor current, output voltage, duty ratio, and switching frequency. Depending on the semiconductor switch's switching condition, the boost converter can function in one of two modes. The inductor stores energy from the input source when the switch is activated. The output voltage rises above the input voltage level when the switch is turned off because the stored energy is transmitted to the load via the diode and capacitor. Because the converter contains switching elements, its behaviour is nonlinear in nature. For control and stability studies, techniques such as state-space averaging and small-signal modelling are commonly used to obtain a simplified dynamic model. These methods make it possible to derive transfer functions suitable for controller design and stability analysis.

In this thesis, mathematical modelling of the DC to DC boost converter is carried out to study its dynamic performance and to support the design of PI/PID controllers using the SBL method. The developed model is further utilized for simulation and verification in MATLAB/Simulink.

$$Vo = \frac{Vin}{1-D} = \frac{24}{1-0.782} = 110$$

(2.1)

The boost converter's optimal voltage gain is shown in the equation above, Vo where denotes the output voltage, Vin represents the input voltage, and D is the duty cycle.

2.2 Design of DC–DC Boost Converter

The purpose of the boost converter is to raise the input DC voltage from 24 V to 110 V for a power rating of 100 W. The converter parameters are selected to ensure continuous conduction mode operation with low ripple and improved stability.

2.2.1 Output Current

The output current is determined from the output power and output voltage relation as

$$Iout = \frac{Pout}{Vout} \tag{2.2}$$

Substituting the design values,

$$Iout = \frac{100}{110} = 0.91\,\text{A}$$

Thus, the converter delivers approximately 0.91 a load current at the output.

2.2.2 Input Current and Average Inductor Current

$$Pin = \frac{Pout}{\eta} \tag{2.3}$$

$$Pin = \frac{100}{0.9} = 111.1\,\text{W}$$

The input current is therefore

$$Iin = \frac{Pin}{Vin} = \frac{111.1}{24} = 4.63\,\text{A}$$

In continuous conduction mode of a boost converter the average inductor current and the input current are approximately equal. Hence, $I_L = 4.63$ A

2.2.3 Duty Cycle Calculation

The duty ratio of the boost converter is determined with the voltage conversion relation.

$$D = 1 - \frac{Vin}{Vout} \tag{2.4}$$

Substituting the values,

$D = 1 - \frac{24}{110} = 0.782$ Therefore, the duty cycle required for the converter is 78.2%

2.2.4 Inductor Ripple Current

Typically, 20% to 40% of the input current is chosen for the inductor ripple current. This design takes into account 30% ripple current.

$$\Delta i_L = 0.3 \times I_{in}$$

$$\Delta i_L = 0.3 \times 4.63 = 1.39 \text{ A}$$

This ripple value ensures smooth converter operation with reduced current stress.

2.2.5 Load Resistance

The equivalent load resistance is obtained using the output power equation

$P_O = \frac{V_O^{\,2}}{R}$ Rearranging this, (2.5)

$$R = \frac{V_O^{\,2}}{P_O}$$

$$R = \frac{110^2}{100} = 121\Omega$$

Hence, the effective load resistance is 121 Ω.

2.2.6 Maximum and Minimum Inductor Current

The peak and minimum inductor currents are calculated using the ripple current magnitude

Maximum inductor current

$$I_{\max} = I_L + \frac{\Delta i_L}{2} \tag{2.6}$$

$$I_{\max} = 4.63 + \frac{1.39}{2} = 5.325\,\text{A}$$

Minimum inductor current

$$I_{\min} = I_L - \frac{\Delta_{iL}}{2} = 4.63 - \frac{1.39}{2} = 3.935\,\text{A}$$

(2.7)

These values verify that continuous conduction mode is being used by the converter..

2.2.7 Inductor Design

The minimum inductance required for continuous current operation is expressed as

$$L_{\min} = \frac{D(1-D)^2 R}{2f} \tag{2.8}$$

For practical design purposes, the inductance is selected from the ripple current relation

$$L = \frac{V_{in} D}{f \Delta i_L}$$

(2.9)

Substituting the values,

$$L = \frac{24 \times 0.782}{50000 \times 1.39} = 270\mu\,\text{H}$$

A standard inductor value of 330μH is selected to ensure reliable continuous conduction operation. The chosen inductor should possess a current rating greater than 7 A with a ferrite core structure to minimize core losses.

2.2.8 Output Capacitor Design

The output capacitor is selected based on the permissible output voltage ripple.

$$C_{out} = \frac{I_{out} D}{f_s \Delta Vout} \tag{2.10}$$

Substituting the design values,

$$C_{out} = 2.58\mu\,\text{F}$$

Since this represents the minimum capacitance value, a practical capacitor value of 100 μF is selected to reduce output voltage ripple and improve transient response. A low ESR capacitor rated above 150 V is preferred.

2.2.9 MOSFET Selection

The MOSFET voltage rating must exceed the output voltage with sufficient safety margin.

$V_{DS} \geq 1.3 \times V_{out}$

$V_{DS} \geq 143\,\text{V use} \geq 150\text{V}$

Therefore, a MOSFET with voltage rating greater than or equal to 150 V is selected.

The peak current through the switch is

Current rating ≥ Peak inductor current

$I_{in} + \frac{\Delta i_L}{2} = 5.33\,\text{A}$

An N-channel MOSFET with low ON-state resistance and current rating above 7 A is suitable for the design.

PWM Controller - UC3845

Gate driver - (9-12) V use (TC4420)/UCC27511

2.2.10 Diode Selection

The boost diode should withstand high reverse voltage and fast switching operation. Therefore, a fast recovery diode with voltage rating above 200 V and current rating above 5 A is selected for reliable operation.

Table 2.1: Boost Converter Parameters Table

Parameter	Value
Input voltage (V_{in})	24V
Output voltage (V_O)	110V
Output Power (P_O)	100W
Switching Frequency(f_s)	50kHz
Duty Cycle (D)	0.782
Inductor (L)	$330\,\mu$H
Capacitor (C)	$100\,\mu$F
Load Resistance (R)	$121\,\Omega$

2.3 Small Signal Analysis of Boost Converter

2.3.1 Mode 1 Operation (Switch ON)

The diode is reverse biased and the inductor stores energy from the source when the switch is turned on. Applying Kirchhoff's Voltage Law,

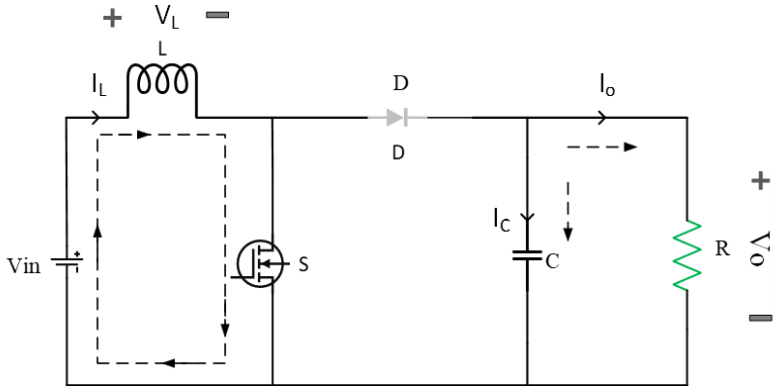

Fig 2.1: Boost converter mode 1

$$-v_{in} + v_L = 0 \quad (v_o = v_c) \tag{2.11}$$

$$L\frac{di_L}{dt} = v_{in}$$

$$\frac{di_L}{dt} = \frac{v_{in}}{L} \tag{2.12}$$

Applying Kirchhoff's Current Law at the output side,

$$i_C + i_O = 0 \tag{2.13}$$

$$i_C = -i_O$$

$$C\frac{dv_c}{dt} = -\frac{v_c}{R} \quad \left(i_o = \frac{v_o}{R} = \frac{v_c}{R} \right)$$

$$\frac{dv_c}{dt} = -\frac{v_c}{RC} \tag{2.14}$$

2.3.2 Mode 2 Operation (Switch OFF)

With the switch OFF the diode is in conductive mode and the stored energy in the inductor is given to the load and the charge of the capacitor.

Applying KVL,

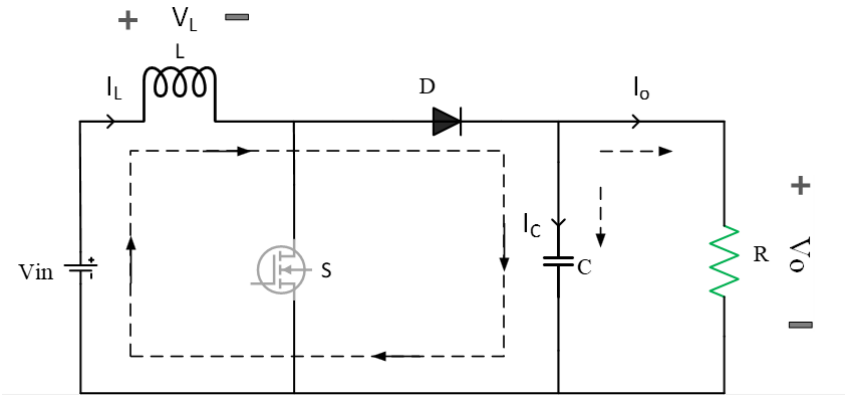

Fig 2.2: Boost converter mode 2

$$-v_{in} + v_L + v_c = 0 \tag{2.15}$$

$$v_L = v_{in} - v_c$$

Using the inductor equation,

$$L\frac{di_L}{dt} = v_{in} - v_c$$

$$\frac{di_L}{dt} = \frac{v_{in}}{L} - \frac{v_c}{L} \tag{2.16}$$

Applying KCL,

$$i_L = i_c + i_o \quad (\, i_D = i_c + i_o\,) \tag{2.17}$$

$$i_c = i_L - i_o \quad (i_o = \frac{v_o}{R} = \frac{v_c}{R})$$

$$\frac{dv_c}{dt} = \frac{i_L}{C} - \frac{v_c}{RC} \tag{2.18}$$

2.3.3 State Space Averaged Model of Boost Converter

The state-space averaging technique combines both operating modes using duty ratio weighting. The averaged inductor current equation becomes

Using equation (2.12) $\times dT$ and equation (2.16) $\times(1-d)T$ and adding both equation we get,

$$\bar{d}T\frac{d\bar{i}_L}{dt} + (1-\bar{d})T\frac{d\bar{i}_L}{dt} = \bar{d}T\frac{v_{in}}{L} + (1-\bar{d})T\frac{v_{in}}{L} - (1-\bar{d})T\frac{\bar{v}_c}{L} \tag{2.19}$$

$$\bar{d}\frac{(d\bar{i}_L)}{dt} + \frac{d\bar{i}_L}{dt} - \bar{d}\frac{(d\bar{i}_L)}{dt} = \bar{d}\frac{v_{in}}{L} - \frac{\bar{v}_c}{L} + \bar{d}\frac{\bar{v}_c}{L} + \frac{v_{in}}{L} - \bar{d}\frac{v_{in}}{L}$$

$$\frac{d\bar{i}_L}{dt} = \frac{v_{in}}{L} - (1-\bar{d})\frac{\bar{v}_c}{L} \tag{2.20}$$

From equation (2.14) $\times dT$ and equation (2.18) $\times(1-d)T$ and adding both equation we get,

$$\bar{d}T\frac{d\bar{v}_c}{dt} + (1-\bar{d})T\frac{d\bar{v}_c}{dt} = -\bar{d}T\frac{\bar{v}_c}{RC} + (1-\bar{d})T\frac{\bar{i}_L}{C} - (1-\bar{d})T\frac{\bar{v}_c}{RC}$$

$$\frac{d\bar{v}_c}{dt} = -\bar{d}\frac{\bar{v}_c}{RC} + (1-\bar{d})\frac{\bar{i}_L}{C} - \frac{\bar{v}_c}{RC} + \bar{d}\frac{\bar{v}_c}{RC}$$

$$\frac{d\bar{v}_c}{dt} = (1-\bar{d})\frac{\bar{i}_L}{C} - \frac{\bar{v}_c}{RC} \tag{2.21}$$

2.3.4 Perturbation and Linearization of Boost Converter

To obtain the small signal model of the boost converter, perturbation quantities are introduced around the steady-state operating point. The inductor current, capacitor voltage, and duty cycle are represented as the sum of steady-state values and small AC perturbations as follows

$$\begin{aligned} \bar{i}_L &= I_L + \hat{i}_L \\ \bar{v}_c &= V_c + \hat{v}_c \\ \bar{d} &= D + \hat{d} \end{aligned} \tag{2.22}$$

where I_L, V_c and D represent the steady-state quantities,

$\hat{i}_L$, $\hat{v}_c$ and $\hat{d}$ represent small perturbations around the operating point.

Linearization of Equation (2.17)

The averaged inductor current equation is given by

$$\frac{d\bar{i}_L}{dt} = \frac{V_{in}}{L} - \frac{(1-\bar{d})\bar{v}_c}{L}$$

substituting the perturbation quantities,

$$\frac{d(I_L + \hat{i}_L)}{dt} = \frac{V_{in}}{L} - \frac{[1-(D+\hat{d})](V_c + \hat{v}_c)}{L}$$

expanding the above equation,

$$\frac{dI_L}{dt} + \frac{d\hat{i}_L}{dt} = \frac{V_{in}}{L} - \frac{(1-D)V_c}{L} + \frac{\hat{d}V_c}{L} - \frac{(1-D)\hat{v}_c}{L} + \frac{\hat{d}\hat{v}_c}{L}$$

The term $\frac{\hat{d}\hat{v}_c}{L}$ is a higher-order perturbation term and is neglected during linearization because the perturbation quantities are very small.

Therefore, the equation becomes

$$\frac{dI_L}{dt}+\frac{d\hat{i}_L}{dt}=\frac{V_{in}}{L}-\frac{(1-D)V_c}{L}+\frac{\hat{d}V_c}{L}-\frac{(1-D)\hat{v}_c}{L} \tag{2.23}$$

Steady-State DC Equation

Comparing the DC terms,

$$\frac{dI_L}{dt}=-\frac{(1-D)V_c}{L}+\frac{V_{in}}{L} \tag{2.24}$$

Under steady-state conditions,

$$\frac{dI_L}{dt}=0$$

hence, $\frac{(1-D)V_c}{L}=\frac{V_{in}}{L}$ which gives

$V_o=\frac{V_{in}}{1-D}$ Since $V_c=V_o$ the output voltage relation of the boost converter is obtained.

Linearization of Equation (2.20)

the averaged capacitor voltage equation is $\frac{d\overline{v}_c}{dt}=\frac{(1-\overline{d})\overline{i}_L}{C}-\frac{\overline{v}_c}{RC}$

substituting perturbation quantities

$$\frac{d(V_c+\hat{v}_c)}{dt}=\frac{[1-(D+\hat{d})](I_L+\hat{i}_L)}{C}-\frac{V_c+\hat{v}_c}{RC} \tag{2.25}$$

expanding,

$$\frac{dV_c}{dt}+\frac{d\hat{v}_c}{dt}=\frac{(1-D)I_L}{C}-\frac{\hat{d}I_L}{C}+\frac{(1-D)\hat{i}_L}{C}-\frac{\hat{i}_L\hat{d}}{C}-\frac{V_c}{RC}-\frac{\hat{v}_c}{RC}$$

The higher -order term $\frac{\hat{i}_L\hat{d}}{C}$ is neglected during linearization.

thus, $$\frac{dV_c}{dt}+\frac{d\hat{v}_c}{dt}=\frac{(1-D)I_L}{C}-\frac{\hat{d}I_L}{C}+\frac{(1-D)\hat{i}_L}{C}-\frac{V_c}{RC}-\frac{\hat{v}_c}{RC} \tag{2.26}$$

Steady - State Capacitor Equation

comparing the DC terms,

$$\frac{dV_c}{dt} = \frac{(1-D)I_L}{C} - \frac{V_c}{RC} \tag{2.27}$$

At steady state,

$$\frac{dV_c}{dt} = 0$$

Hence, $\frac{(1-D)I_L}{C} = \frac{V_c}{RC}$ which gives

$I_L = \frac{V_c}{(1-D)R}$ Since $V_c = V_o$ and $I_o = \frac{V_o}{R}$ therefore,

$I_L = \frac{I_o}{1-D}$ This equation represents the average inductor current relation of the boost converter.

2.3.5 Small Signal AC Model

After comparing the AC terms from the linearized equations, the small signal equations are obtained.

The inductor current perturbation equation becomes

$$\frac{d\hat{i}_L}{dt} = -\frac{(1-D)\hat{v}_c}{L} + \frac{V_c\hat{d}}{L}$$

Similarly, the capacitor voltage perturbation equation becomes

$$\frac{d\hat{v}_c}{dt} = \frac{(1-D)\hat{i}_L}{C} - \frac{I_L\hat{d}}{C} - \frac{\hat{v}_c}{RC}$$

These equations form the small signal AC model of the boost converter.

2.3.6 Laplace Transform of Small Signal Equations

Applying Laplace transform,

$$Ls\hat{i}_L(s) = -(1-D)\hat{v}_c(s) + V_c\hat{d}(s) \tag{2.28}$$

$$Cs\hat{v}_c(s) = (1-D)\hat{i}_L(s) - I_L\hat{d}(s) - \frac{\hat{v}_c(s)}{R} \tag{2.29}$$

2.3.7 Control - to- Output Voltage Transfer Function

From the (2.22) equation

$$\hat{i}_L(s) = \frac{-(1-D)\hat{v}_c(s) + V_c\hat{d}(s)}{Ls}$$

Substituting into the (2.23) equation,

$$C s \hat{v}_c(s) = (1-D)\left(\frac{-(1-D)\hat{v}_c(s) + V_c \hat{d}(s)}{Ls} \right) - I_L \hat{d}(s) - \frac{\hat{v}_c(s)}{R} \tag{2.30}$$

Using $I_L = \frac{V_c}{(1-D)R}$ and simplifying,

$$\hat{v}_c(s)\left(Cs + \frac{(1-D)^2}{Ls} + \frac{1}{R} \right) = \hat{d}(s)\left(\frac{(1-D)V_c}{Ls} - \frac{V_c}{(1-D)R} \right) \tag{2.31}$$

Therefore, the control-to-output transfer function becomes

$$\frac{\hat{v}_o(s)}{\hat{d}(s)} = \frac{V_o\left((1-D) - \frac{Ls}{R(1-D)} \right)}{LCs^2 + \frac{Ls}{R} + (1-D)^2} \tag{2.32}$$

This transfer function represents the relationship between duty cycle variation and output voltage response of the boost converter.

2.3.8 Control - to - Inductor Current Transfer Function

Eliminating capacitor voltage from the small signal equations yields

$$\hat{d}(s)\left(V_o Cs + \frac{2V_o}{R} \right) = \hat{i}_L(s)\left(LCs^2 + \frac{Ls}{R} + (1-D)^2 \right) \tag{2.33}$$

Hence, the transfer function relating duty cycle perturbation to inductor current is obtained as

$$\frac{\hat{i}_L(s)}{\hat{d}(s)} = \frac{V_o Cs + \frac{2V_o}{R}}{LCs^2 + \frac{Ls}{R} + (1-D)^2} \tag{2.34}$$

The derived transfer functions are useful for controller design, stability analysis, and performance evaluation of the DC-DC boost converter system.

Control -to- Output Voltage Transfer Function

The transfer function of the control-to-output voltage of the proposed DC-DC boost converter is expressed as

$$\frac{\hat{v}_o(s)}{\hat{d}(s)} = \frac{V_o\left((1-D) - \frac{Ls}{R(1-D)} \right)}{LCs^2 + \frac{Ls}{R} + (1-D)^2}$$

The converter parameters used in the analysis are listed below

Output Voltage, V_o =110 V

Inductor, L=330 μ H

Capacitance, C=100 μ F

Load resistance, R=121 Ω

Duty cycle, D=0.782 The value of (1-D) is calculated as 1-D=1- 0.782 =0.218

Substituting these values into the transfer function gives

$$\frac{\hat{v}_o(s)}{\hat{d}(s)} = \frac{110\left(0.218 - \frac{330\times10^{-6}}{121\times0.218}\right)}{(330\times10^{-6}\times100\times10^{-6})s^2 + \frac{330\times10^{-6}}{121} + (0.218)^2} \tag{2.35}$$

After simplification,

$$\frac{\hat{v}_o(s)}{\hat{d}(s)} = \frac{23.98 - 0.001376s}{3.3\times10^{-8}s^2 + 2.73\times10^{-6}s + 0.0475} \tag{2.36}$$

The obtained transfer function describes the relationship between variations in duty cycle and the corresponding output voltage response of the boost converter.

Control-to-Inductor Current Transfer Function

The control-to-inductor current transfer function of the boost converter is represented by

$$\frac{\hat{i}_L(s)}{\hat{d}(s)} = \frac{V_oCs + \frac{2V_o}{R}}{LCs^2 + \frac{Ls}{R} + (1-D)^2}$$

Substituting the converter parameters,

Output voltage, V_o =110 V

Inductance, L=330 μ H

Capacitance, C=100 μ F

Load resistance, R=121 Ω

Duty cycle, D=0.782 the equation becomes

$$\frac{\hat{i}_L(s)}{\hat{d}(s)} = \frac{110\times100\times10^{-6}s + \frac{2\times110}{121}}{(330\times10^{-6}\times100\times10^{-6})s^2 + \frac{330\times10^{-6}}{121} + (1-0.782)^2} \tag{2.37}$$

thus, the simplified transfer function becomes

$$\frac{\hat{i}_L(s)}{\hat{d}(s)} = \frac{0.011s + 1.818}{3.3\times10^{-8}s^2 + 2.73\times10^{-6}s + 0.0475}$$

Hence, the final control-to-inductor current transfer function is expressed as

$$\frac{\hat{i}_L(s)}{\hat{d}(s)} = \frac{0.011s + 1.818}{3.3\times10^{-8}s^2 + 2.73\times10^{-6}s + 0.0475} \tag{2.38}$$

This transfer function represents the dynamic relationship between duty cycle variation and inductor current response. It is useful for analyzing converter stability and designing suitable control strategies for improved dynamic performance.

CHAPTER 3

Theoretical concepts of the Stability Boundary Locus (SBL)

3.1 Introduction

Stability Boundary Locus is a graphical and analytical method that can be used to analyze the range of the stabilizing parameters of controllers in linear control systems. The SBL is widely utilized in design problems of PI and PID controllers due to its ability to provide a systematic way of finding stabilizing regions in the plane of controller parameters [15]. Compared to traditional methods for controller tuning, the SBL method gives a clear idea of the range of the stabilizing parameters without having to rely heavily on empirical tuning.

In power electronic systems like DC-DC boost converters, it is extremely important to perform an accurate stability analysis since their behavior depends very much on parameter values and disturbances. As such, SBL is an efficient method of obtaining controller parameters that contribute to stability and robustness. Stability Boundary Locus (SBL) is an analytical method of obtaining the entire range of stabilizing parameters of the controller. SBL method involves analysis of the closed-loop system's characteristic equation utilising frequency domain methods. The method involves plotting stability boundaries of the controller in the controller parameters plane and thereby obtaining stabilizing and non-stabilizing regions of the controller [18]. SBL method becomes increasingly popular due to high accuracy, efficiency and straight forwardness of calculations regarding different operating conditions and changes in the system parameters. SBL is the proper approach which helps in the process of parameter choice to attain more desirable dynamic behavior with respect to reduction of overshoot, achieving steady-state conditions faster, and disturbances rejection properties. In case of the DC-DC boost converter the usage of such approach helps in obtaining more stable control system operations depending on changing operating conditions [19].

In this chapter we will be analyzing theoretical background of the SBL method as well as application of SBL to PI controller design for DC-DC boost converters.

3.2 Flow chart for computing Stabilizing PI Controller Using Stability Boundary Locus

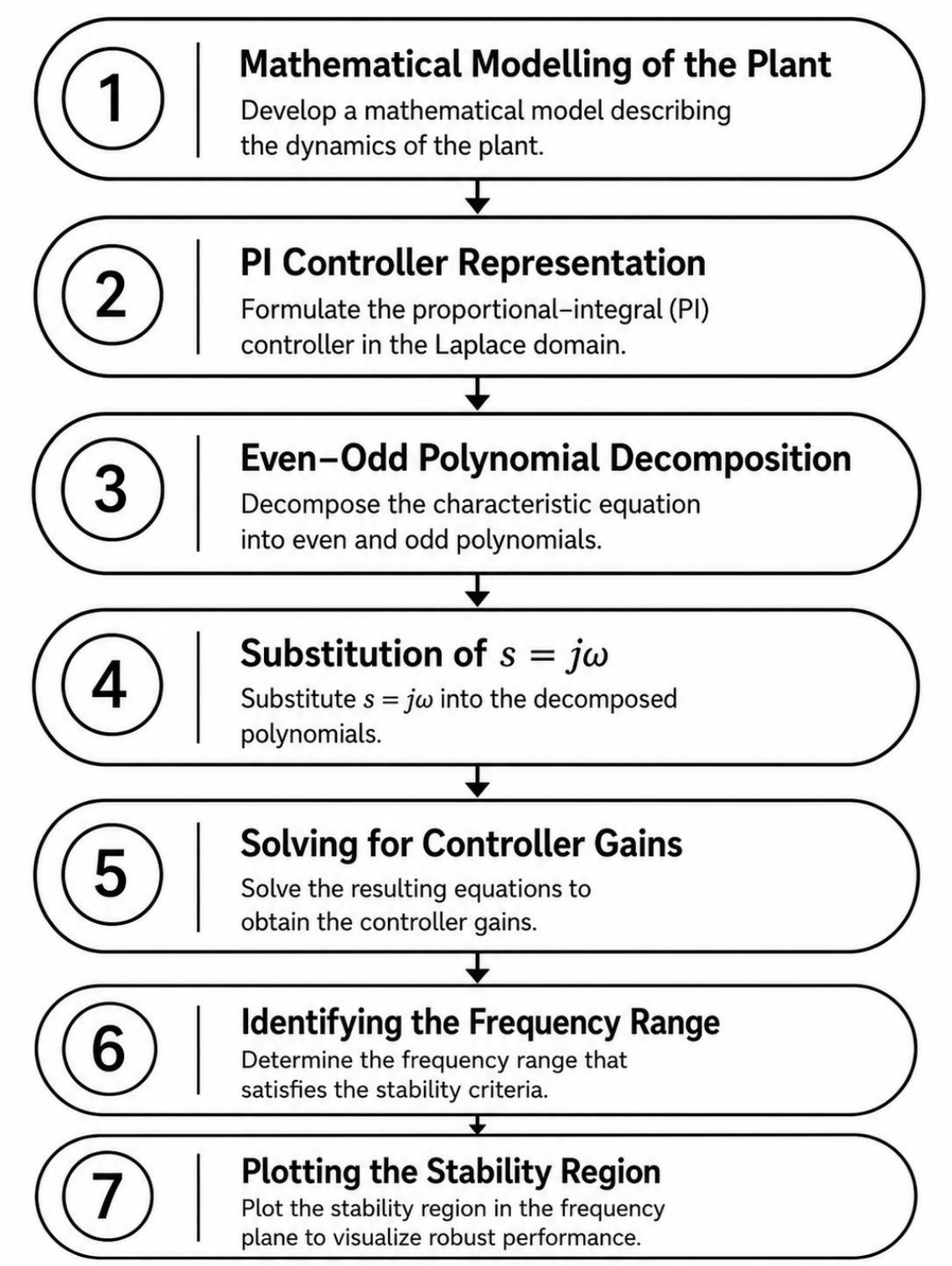

Fig3.1: Flow chart for stabilizing PI controller using SBL

3.3 Mathematical Representation of the Plant

Consider a single-input single-output (SISO) feedback control system consisting of a plant and a PI controller. The plant transfer function is represented as

$$G(s) = \frac{N(s)}{D(s)} \tag{3.1}$$

Where $N(s)$ and $D(s)$ denote the numerator and denominator polynomials of the system. The PI controller transfer function is expressed as

$$C(s) = k_p + \frac{k_i}{s} = \frac{k_p s + k_i}{s} \tag{3.2}$$

Where

k_p and k_i denote the proportional and integral gains .

3.4 Closed -Loop Characteristic Equation

The characteristic equation of a unity feedback system is given by

$$1 + C(s)G(s) = 0 \tag{3.3}$$

The system's closed loop characteristics polynomial can be expressed as

$$\triangle(s) = [k_i N_e(-\omega^2) - k_p \omega^2 N_o(-\omega^2) - \omega^2 D_o(-\omega^2)] + j[k_p \omega N_e(-\omega^2) + k_i \omega N_o(-\omega^2) + \omega D_e(-\omega^2)] = 0$$

The roots of this equation determine the stability of the system. A system is considered to be stable when all characteristic roots lie in the left half of the complex plane. Therefore, suitable controller gains must be selected to satisfy this stability condition [15]. To simplify the stability analysis, the numerator and denominator polynomials are decomposed into even and odd components. This decomposition helps separate the characteristic equation into real and imaginary parts.

3.5 Even-Odd Polynomial Decomposition

The frequency-domain analysis is performed by substituting

$s = j\omega$

Where $j = \sqrt{-1}$

ω is the angular frequency

After substitution, the plant transfer function becomes

(3.4)

Where $G(j\omega) = \dfrac{N_e(-\omega^2) + j\omega N_o(-\omega^2)}{D_e(-\omega^2) + j\omega D_o(-\omega^2)}$

- $N_e(-\omega^2)$ and $N_o(-\omega^2)$ are the even and odd parts of the numerator polynomial
- $D_e(-\omega^2)$ and $D_o(-\omega^2)$ are the even and odd parts of the denominator polynomial

Then, equating the real and imaginary parts of $\triangle(s)$ to zero, one obtains

$$k_p(-\omega^2 N_o(-\omega^2)) + k_i(N_e(-\omega^2)) = \omega^2 D_o(-\omega^2) \tag{3.5}$$

And

$$k_p(\omega N_e(-\omega^2)) + k_i(\omega N_o(-\omega^2)) = -\omega D_e(-\omega^2) \tag{3.6}$$

Let

$$Q(\omega) = -\omega^2 N_o(-\omega^2),\ R(\omega) = N_e(-\omega^2)$$

$$S(\omega) = \omega N_e(-\omega^2),\ U(\omega) = \omega N_o(-\omega^2)$$

$$X(\omega) = \omega^2 D_o(-\omega^2),\ Y(\omega) = -\omega D_e(-\omega^2) \tag{3.7}$$

This transformation converts the characteristic equation into a frequency-dependent form, which is easier to analyze graphically [15].

3.6 Formation of Stability Equations

After substituting $s = j\omega$ the characteristic equation separated into real and imaginary components. Equating these components to zero produces two equations

$$k_p Q(\omega) + k_i R(\omega) = X(\omega)$$

And

$$k_p S(\omega) + k_i U(\omega) = Y(\omega)$$

Where

- $Q(\omega)$, $R(\omega)$, $S(\omega)$, and $U(\omega)$ are frequency-dependent functions derived from the numerator polynomial
- $X(\omega)$ and $Y(\omega)$ are functions obtained from the denominator polynomial

These equations form the mathematical basis of the Stability Boundary Locus method [15]

3.7 Determination of PI Controller Parameters

The simultaneous equations are solved to obtain the proportional and integral gains as functions of frequency .The proportional gain is given by

Then Eq. (3.5) and Eq.(3.6) can be written as

$$k_p Q(\omega) + k_i R(\omega) = X(\omega)$$

$$k_p S(\omega) + k_i U(\omega) = Y(\omega) \tag{3.8}$$

From these equation

$$k_p = \frac{X(\omega)U(\omega) - Y(\omega)R(\omega)}{Q(\omega)U(\omega) - R(\omega)S(\omega)} \tag{3.9}$$

And

$$k_i = \frac{Y(\omega)Q(\omega) - X(\omega)S(\omega)}{Q(\omega)U(\omega) - R(\omega)S(\omega)} \tag{3.10}$$

Similarly, the integral gain is expressed as

$$k_p = \frac{X(\omega)U(\omega) - Y(\omega)R(\omega)}{Q(\omega)U(\omega) - R(\omega)S(\omega)} \quad \& \quad k_i = \frac{Y(\omega)Q(\omega) - X(\omega)S(\omega)}{Q(\omega)U(\omega) - R(\omega)S(\omega)} \tag{3.11}$$

These equations generate the controller parameters corresponding to different frequency values [15]

3.8 Stability Boundary Locus in the Parameter Plane

The angular frequency ω is varied over a specified range, and the corresponding values of k_p and k_i are calculated. Plotting these values forms the Stability Boundary Locus (SBL) in the (k_p, k_i) parameter plane. The parameter plane is divided into stable and unstable areas by the produced curves. From each region, a test point is chosen, and the stability of the associated closed-loop system is verified using stability criteria such as pole location analysis or the Hurwitz criterion [15]. The region that satisfies the stability condition represents the stabilizing region of the PI controller parameters.

3.9 Stability Verification Procedure

The paper explains that not all regions formed by the stability boundary curves are stable. Therefore to confirm the stability of the system, a test point is chosen from each region. If the chosen point generates poles in the complex plane's right half, the region is

unstable. Conversely, if all poles lie in the left half plane, the region is considered stable [15] This procedure allows accurate identification of all stabilizing values of the controller parameters.

3.10 Frequency Gridding and Computational Improvement

One limitation of the SBL method is frequency gridding, where a large number of frequency points are required to generate accurate stability boundaries. Excessive gridding increases computational complexity. To overcome this issue, the paper introduces a Nyquist-based approach in which only frequencies satisfying

$\mathrm{Im}[G(j\omega)] = 0$ are considered [15]

This significantly reduces computation time while preserving accuracy.

3.11 Implementation of Stability Boundary Locus Method for Boost Converter

Boost converter control-to-output transfer function

Using equation (2.26)

$$G(s) = \frac{\hat{v}_o(s)}{\hat{d}(s)} = \frac{23.98 - 0.001376s}{3.3\times10^{-8}s^2 + 2.73\times10^{-6}s + 0.0475}$$

And PI controller is

$$C(s) = k_p + \frac{k_i}{s} = \frac{k_p s + k_i}{s}$$

Close Loop Characteristic Equation

For unity feedback

$1 + C(s)G(s) = 0$

Substitute the boost converter control-to-output transfer function

$$1 + \left(K_p + \frac{K_i}{s}\right)\frac{23.98 - 0.001376s}{3.3\times10^{-8}s^2 + 2.73\times10^{-5}s + 0.0475} = 0 \qquad (3.12)$$

multiplying throughout in this equation

$$s(3.3\times10^{-8}s^2 + 2.73\times10^{-5}s + 0.0475) + (K_p s + K_i)(23.98 - 0.001376s) = 0$$

expanding the equation.

$$3.3\times10^{-8}s^3+2.73\times10^{-5}s^2+0.0475s+23.98K_ps-0.001376K_ps^2+23.98K_i-0.001376K_is=0$$

the characteristic equation becomes like this

$$3.3\times10^{-8}s^3+(2.73\times10^{-5}-0.001376K_p)s^2+(0.0475+23.98K_p-0.001376K_i)s+23.98K_i=0$$

For stability boundary substitute $s=j\omega$,

$$3.3\times10^{-8}(j\omega)^3+(2.73\times10^{-5}-0.001376K_p)(j\omega)^2+(0.0475+23.98K_p-0.001376K_i)(j\omega)+23.98K_i=0$$

$$-3.3\times10^{-8}j\omega^3-(2.73\times10^{-5}-0.001376K_p)\omega^2+j\omega(0.0475+23.98K_p-0.001376K_i)+23.98K_i=0$$

separate real and imaginary parts of above equation

Real part is this

$$-(2.73\times10^{-5}-0.001376K_p)\omega^2+23.98K_i=0$$

hence

$$K_i=\frac{(2.73\times10^{-5}-0.001376K_p)\omega^2}{23.98}$$

(3.13)

and Imaginary part is this

$$-3.3\times10^{-8}\omega^3+\omega(0.0475+23.98K_p-0.001376K_i)=0$$

diving by ω

$$-3.3\times10^{-8}\omega^2+0.0475+23.98K_p-0.001376K_i=0$$

substitute expression of K_i

$$-3.3\times10^{-8}\omega^2+0.0475+23.98K_p-0.001376\left[\frac{(2.73\times10^{-5}-0.001376K_p)\omega^2}{23.98}\right]=0$$

Therefore

$$K_p=\frac{3.3\times10^{-8}\omega^2-0.0475+\left(\frac{0.001376(2.73\times10^{-5})\omega^2}{23.98}\right)}{\left(23.98+\frac{(0.001376)^2\omega^2}{23.98}\right)} \qquad (3.14)$$

$$K_p(\omega)=\frac{3.4565\times10^{-8}\omega^2-0.0475}{23.98+7.893\times10^{-8}\omega^2} \qquad (3.15)$$

and

$$K_i = \frac{(2.73\times10^{-5} - 0.001376K_p)\omega^2}{23.98} \tag{3.16}$$

after simplify this equation becomes as

$$K_i(\omega) = \frac{1.138\times10^{-6}\omega^2 - 1.984\times10^{-12}\omega^4}{23.98 + 7.893\times10^{-8}\omega^2}$$

Final Stability Boundary Locus Equations

The SBL equation for the boost converter is

$$K_p(\omega) = \frac{3.4565\times10^{-8}\omega^2 - 0.0475}{23.98 + 7.893\times10^{-8}\omega^2} \tag{3.17}$$

and

$$K_i(\omega) = \frac{1.138\times10^{-6}\omega^2 - 1.984\times10^{-12}\omega^4}{23.98 + 7.893\times10^{-8}\omega^2} \tag{3.18}$$

equations (3.15) and (3.16) can be used in MATLAB to plot the SBL in the (K_p, K_i) plane.

Boost converter control-to-inductor current transfer function

using equation (2.27)

$$\frac{\hat{i}_L(s)}{\hat{d}(s)} = \frac{0.011s + 1.818}{3.3\times10^{-8}s^2 + 2.73\times10^{-6}s + 0.0475}$$

general form of PI controller is

$$C(s) = k_p + \frac{k_i}{s} = \frac{k_p s + k_i}{s}$$

Close Loop Characteristic Equation

for unity feedback close loop system

$$1 + C(s)G(s) = 0$$

put the boost converter control-to-inductor current transfer function in this equation

$$1+\left(K_p+\frac{K_i}{s}\right)\frac{0.011s+1.818}{3.3\times10^{-8}s^2+2.73\times10^{-6}s+0.0475}=0 \tag{3.19}$$

closed loop Characteristic Equation

$$1+\frac{\left(K_p+\frac{K_i}{s}\right)(0.011s+1.818)}{3.3\times10^{-8}s^2+2.73\times10^{-6}s+0.0475}=0 \tag{3.20}$$

multiply entire equation by s and expanding

$$3.3\times10^{-8}s^3+2.73\times10^{-6}s^2+0.0475s+(K_ps+K_i)(0.011s+1.818)=0$$

substitute $s=j\omega$

$$3.3\times10^{-8}(-j\omega^3)+(2.73\times10^{-6}+0.011K_p)(-\omega^2)+j\omega(0.0475+1.818K_p+0.011K_i)+1.818K_i=0$$

separate real and imaginary Parts of the above equation

Real part is this

$$-\omega^2(2.73\times10^{-6}+0.011K_p)+1.818K_i=0$$

and

$$K_i=\frac{\omega^2(2.73\times10^{-6}+0.011K_p)}{1.818} \tag{3.21}$$

Imaginary part is this

$$-3.3\times10^{-8}\omega^3+\omega(0.0475+1.818K_p+0.011K_i)=0$$

$$K_p=\frac{3.3\times10^{-8}\omega^2-0.0475-0.011K_i}{1.818} \tag{3.22}$$

put these values into imaginary equation

$$0.0475+1.818K_p+0.011\left(\frac{\omega^2(2.73\times10^{-6}+0.011K_p)}{1.818}\right)=3.3\times10^{-8}\omega^2 \tag{3.23}$$

after simplification

$$K_p(\omega) = \frac{3.3\times10^{-8}\omega^2 - \dfrac{3.003\times10^{-8}\omega^2}{1.818} - 0.0475}{\left(1.818 + \dfrac{0.000121\omega^2}{1.818}\right)} \tag{3.24}$$

$$K_p(\omega) = \frac{1.6482\times10^{-8}\omega^2 - 0.0475}{1.818 + 6.6557\times10^{-5}\omega^2} \tag{3.25}$$

place into K_i equation

$$K_i = \frac{\omega^2}{1.818}\left[2.73\times10^{-6} + 0.011\left(\frac{1.6482\times10^{-8}\omega^2 - 0.0475}{1.818 + 6.6557\times10^{-5}\omega^2}\right)\right] \tag{3.26}$$

after simplification

$$K_i(\omega) = \frac{3.63\times10^{-10}\omega^4 - 0.000517538\omega^2}{3.305124 + 1.209\times10^{-4}\omega^2} \tag{3.27}$$

final Stability Locus Equation

$$K_p(\omega) = \frac{1.6482\times10^{-8}\omega^2 - 0.0475}{1.818 + 6.6557\times10^{-5}\omega^2} \tag{3.28}$$

And

$$K_i(\omega) = \frac{3.63\times10^{-10}\omega^4 - 0.000517538\omega^2}{3.305124 + 1.209\times10^{-4}\omega^2} \tag{3.29}$$

above equation are the SBL equation used for MATLAB plotting.

3.12 Advantages of the Stability Boundary Locus Method

Several practical benefits can be obtained from utilizing the Stability Boundary Locus (SBL). One of the biggest benefits of applying this method in controller design and stability analysis is the possibility of determining all stabilizing controller gains in one go. This means there will be no need to perform tedious tuning of the controller and complicated guesswork. The other notable characteristic of the SBL is the graphical presentation of the stable and unstable regions within the controller parameter space, making it possible to analyze the stability of the system. As compared to the tuning of the

controllers through optimization techniques, the SBL requires lesser computational effort and faster calculations. Moreover, the method increases the robustness and dynamics of the system by choosing suitable controller parameters to meet stability criteria. The SBL approach can also be used for analysis of relative stability and design of PID controllers. Thanks to advantages, the SBL method is highly suitable for nonlinear control systems and power electronic applications such as DC-DC boost converters [15].

2.13 Application to DC- DC Boost Converter

DC- DC boost converter has nonlinear characteristics and is very sensitive to input voltage, output load and switching operation. These changes may have a profound effect on the stability and overall operation of the converter system. Despite the fact that traditional controller tuning methods are useful, they can not necessarily guarantee reliable operation under different operating conditions because they give little knowledge of the stable operating range of the controller parameters. The SBL method is a systematic and effective way of choosing stabilizing gains of PI controllers. The method enables to determine the stable regions in the controller parameter plane, thereby achieving better output voltage regulation, better transient response, higher disturbance rejection, and stable converter operation under various operating conditions. In addition, the graphical representation of the The SBL technique simplifies the controller design and strengthens the system's resistance to parameter variations and outside disruptions. Therefore, the stability analysis and controller design of DC-DC boost converters in the fields of power electronics and renewable energy can benefit greatly from the application of the Stability Boundary Locus approach. [15].

CHAPTER 4
Relative Stability Analysis Using Stability Boundary Locus Method

4.1 Introduction

In control system design, obtaining stability alone is not enough for satisfactory operation. The system should also be responsive and fluid with respect to varying operating conditions. This requirement is referred to as relative stability. It provides information regarding distance of closed-loop poles from imaginary axis of the complex plane. Relative stability is an important property in the case of DC- DC boost converters, since the converter is very sensitive to changes in the load and the input voltage source. The converter can oscillate, have high overshoot and slow transient response if poles are within a close proximity to the imaginary axis. Hence, the dynamic response of a controller should be designed to have its poles further into LHP to enhance overall dynamic response to find the controller parameters for a desired stability margin, the SBL method provides a methodical approach. The second approach is to move the stability boundary from the imaginary axis to a desired point in the left half plane. Therefore, better transient performance and better damping characteristics can be obtained

.4.2 Concept of Relative Stability

A system is said to be relatively stable when all closed-loop poles are located sufficiently away from the imaginary axis. The farther the poles lie in the left-half plane, the faster and more stable the system response becomes.

The desired stability condition can be represented by:

From the equation (3.1) and (3.2)

$$\tilde{G}(s) = G(s+\rho) = \frac{N(s+\rho)}{D(s+\rho)} = \frac{\tilde{N}(s)}{\tilde{D}(s)} \tag{4.1}$$

And

$$\tilde{C}(s) = C(s+\rho) = \frac{K_p s + K_p \rho + K_i}{s+\rho} \tag{4.2}$$

Equation (4.1) can be written as

$$\tilde{G}(j\omega) = \frac{\tilde{N}_e(-\omega^2) + j\omega\tilde{N}_o(-\omega^2)}{\tilde{D}_e(-\omega^2) + j\omega\tilde{D}_o(-\omega^2)} \tag{4.3}$$

Then Eq. (3.7) for this becomes

$$Q(\omega) = \rho\tilde{N}_e(-\omega^2) - \omega^2\tilde{N}_o(-\omega^2)$$

$$R(\omega) = \tilde{N}_e(-\omega^2)$$

$$S(\omega) = \omega(\tilde{N}_e(-\omega^2) + \rho\tilde{N}_o(-\omega^2)),\ U(\omega) = \omega\tilde{N}_o(-\omega^2)$$

$$X(\omega) = \omega^2\tilde{D}_o(-\omega^2) - \rho\tilde{D}_e(-\omega^2)$$

$$Y(\omega) = -\omega(\tilde{D}_e(-\omega^2) + \rho\tilde{D}_o(-\omega^2)) \tag{4.4}$$

Using equation (3.11) can be written as

$$k_p = \frac{X(\omega)U(\omega) - Y(\omega)R(\omega)}{Q(\omega)U(\omega) - R(\omega)S(\omega)} \tag{4.5}$$

$$k_i = \frac{Y(\omega)Q(\omega) - X(\omega)S(\omega)}{Q(\omega)U(\omega) - R(\omega)S(\omega)} \tag{4.6}$$

$$k_p = \frac{[\omega^2\tilde{D}_o(-\omega^2) - \rho\tilde{D}_e(-\omega^2)][\omega\tilde{N}_o(-\omega^2)] - [-\omega(\tilde{D}_e(-\omega^2) + \rho\tilde{D}_o(-\omega^2))][\tilde{N}_e(-\omega^2)]}{[\rho\tilde{N}_e(-\omega^2) - \omega^2 N_o(-\omega^2)][\omega\tilde{N}_o(-\omega^2)] - [\tilde{N}_e(-\omega^2)][\omega(\tilde{N}_e(-\omega^2) + \rho\tilde{N}_o(-\omega^2))]} \tag{4.7}$$

$$k_i = \frac{[-\omega(\tilde{D}_e(-\omega^2) + \rho\tilde{D}_o(-\omega^2))][\rho\tilde{N}_e(-\omega^2) - \omega^2\tilde{N}_o(-\omega^2)]}{[\rho\tilde{N}_e(-\omega^2) - \omega^2\tilde{N}_o(-\omega^2)][\omega\tilde{N}_o(-\omega^2)] - [\tilde{N}_e(-\omega^2)][\omega(\tilde{N}_e(-\omega^2) + \rho\tilde{N}_o(-\omega^2))]}$$
$$\frac{-[\omega^2\tilde{D}_o(-\omega^2) - \rho\tilde{D}_e(-\omega^2)][\omega(\tilde{N}_e(-\omega^2) + \rho\tilde{N}_o(-\omega^2))]}{[\rho\tilde{N}_e(-\omega^2) - \omega^2\tilde{N}_o(-\omega^2)][\omega\tilde{N}_o(-\omega^2)] - [\tilde{N}_e(-\omega^2)][\omega(\tilde{N}_e(-\omega^2) + \rho\tilde{N}_o(-\omega^2))]} \tag{4.8}$$

4.3 Mathematical Transformation for Relative Stability

Consider the control - to - output transfer function of boost converter

$$G(s) = \frac{\hat{v}_o(s)}{\hat{d}(s)} = \frac{23.98 - 0.001376s}{3.3\times10^{-8}s^2 + 2.73\times10^{-6}s + 0.0475}$$

First assume $\rho = 0$ then from equation (3.7) and (3.11)

$$K_p(\omega) = \frac{3.4565\times10^{-8}\omega^2 - 0.0475}{23.98 + 7.893\times10^{-8}\omega^2}$$

$$K_i(\omega) = \frac{1.138\times10^{-6}\omega^2 - 1.984\times10^{-12}\omega^4}{23.98 + 7.893\times10^{-8}\omega^2}$$

From equation (4.1) and (4.2)

$$\tilde{G}(s) = G(s+\rho) = \frac{N(s+\rho)}{D(s+\rho)} = \frac{\tilde{N}(s)}{\tilde{D}(s)}$$

$$\tilde{C}(s) = C(s+\rho) = \frac{K_p s + K_p\rho + K_i}{s+\rho}$$

In above equation put $\rho = -0.5$

$$\tilde{G}(s) = G(s-0.5) = \frac{N(s-0.5)}{D(s-0.5)} = \frac{\tilde{N}(s)}{\tilde{D}(s)} \quad (4.9)$$

$$\tilde{C}(s) = C(s+-0.5) = \frac{K_p s - 0.5K_p + K_i}{s-0.5} \quad (4.10)$$

$\tilde{G}(s)$ Consider the control - to - output transfer function of boost converter

$$\tilde{G}(s) = \frac{\tilde{N}(s)}{\tilde{D}(s)} = \frac{23.98 - 0.001376(s-0.5)}{3.3\times10^{-8}(s-0.5)^2 + 2.73\times10^{-6}(s-0.5) + 0.0475} \quad (4.11)$$

Close loop characteristic equation

for unity feedback system

$$1 + \tilde{C}(s)\tilde{G}(s) = 0$$

$$1 + \left(\frac{K_p s - 0.5K_p + K_i}{s-0.5}\right)\left(\frac{23.98 - 0.001376(s-0.5)}{3.3\times10^{-8}(s-0.5)^2 + 2.73\times10^{-6}(s-0.5) + 0.0475}\right) = 0 \quad (4.12)$$

Final closed loop characteristic polynomial

$$3.3\times10^{-8}s^3+(2.6805\times10^{-6}-0.001376K_p)s^2+(0.047497294$$
$$+23.98137K_p-0.001376K_i)s+(-0.02374932-11.990344K_p+23.98066K_i)=0$$

Put $s=j\omega$, separate real and imaginary part of the above equation

real part is this

$$0.001376K_P\omega^2-2.6805\times10^{-6}\omega^2-11.99034K_p+23.98066K_i-0.02374=0$$

imaginary part is this

$$-3.3\times10^{-8}\omega^3+0.0474972\omega+23.9813K_p\omega-0.00137K_i\omega=0$$

$$K_p=\frac{7.9104\times10^{-7}\omega^2-1.13914}{1.8934\times10^{-6}\omega^2+575.095} \tag{4.13}$$

$$K_i=\frac{4.54\times10^{-11}\omega^4-6.78\times10^{-5}\omega^2-2.38\times10^{-5}}{1.8934\times10^{-6}\omega^2+575.095} \tag{4.14}$$

Using above equation (4.13) and equation (4.14) we plot the RBSL plot .

CHAPTER 5

RESULT AND DISCUSSION

The proposed closed-loop controlled boost converter was modelled and simulated in MATLAB/Simulink to evaluate its dynamic and steady- state performance. The system includes an outer voltage control loop and an inner inductor-current loop, both implemented using PI controllers. The simulation was carried out with a 24-V input source, 330-µH inductor, 100-µF output capacitor, and a 121-Ω load.

The output voltage response shows that the converter successfully steps up the input voltage to the desired level. During the transient period, the voltage increases steadily to around 118–120 V, before stabilizing to near the reference voltage. The overshoot is very small and the settling time is acceptable, which means that the PI parameters used for the voltage loop have good dynamic stability. The input/inductor current wave form shows a progressive increase as the duty cycle is increased, to fulfill the output voltage requirement. The steady state value of the current is approximately 4.5-5A, consistent with the theoretical results for the selected boost ratio and load. The current profile doesn't have too much ripple, leading to the conclusion that the profile has been designed to give continuous-conduction-mode (CCM) operation. The simulation results show that the dual-loop control this is a useful method for regulating the boost converter's output voltage. and to maintain the inductor current. Converter has good transient response, controlled overshoot and good steady-state response. These results confirm the design methodology and show the practicality of the proposed PI-based control scheme for using the boost converter in real applications

5.1 Simulation diagram of proposed converter

The MATLAB/Simulink model of the closed loop DC to DC boost converter intended for high voltage output regulation is depicted in this picture. Using a cascaded PI control technique, the converter increases the input supply voltage of 24 V to a regulated output voltage of 110 V. The reference voltage of 110 V is compared with the observed output voltage. A PI controller processes the resulting voltage error to produce the reference current needed to maintain voltage regulation. The measured inductor current and the reference current from the voltage controller are contrasted. The inaccuracy that results from this comparison is used to another PI controller that

determines the required duty ratio for converter switching. The simulation confirms that the controller maintains the output voltage close to the desired reference value while ensuring stable current behavior. Hence, the developed closed-loop boost converter model demonstrates effective voltage regulation and stable operation under the selected operating conditions.

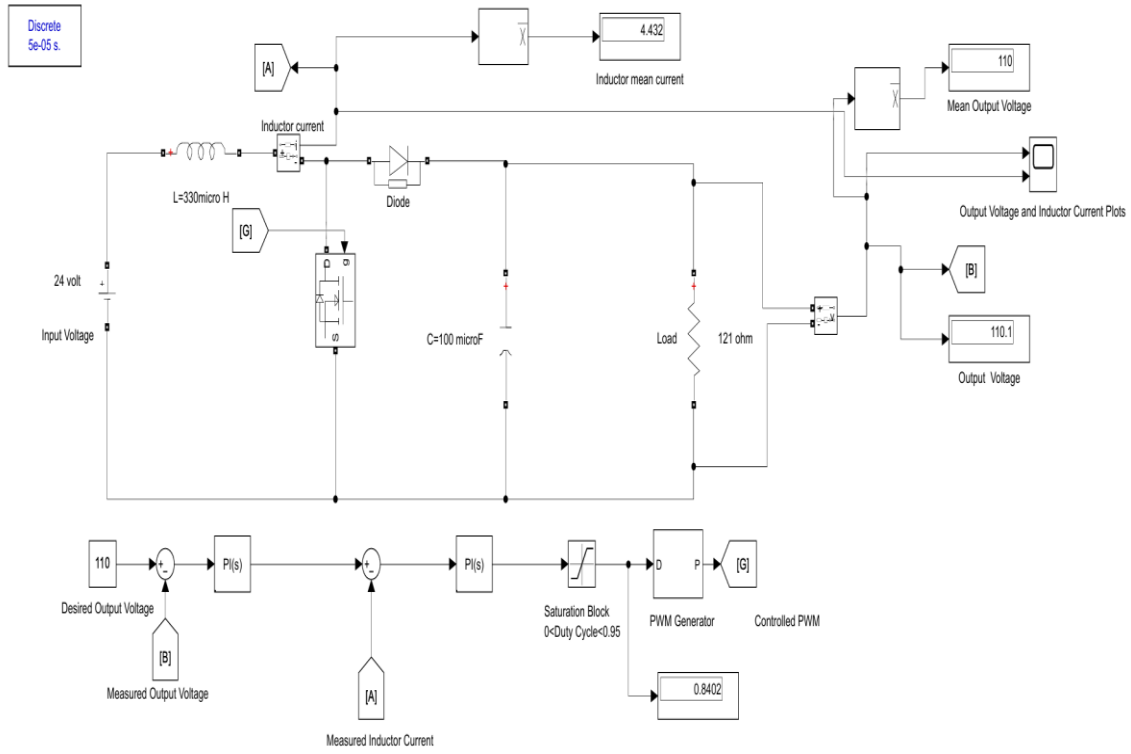

Fig 5.1: Simulation diagram of boost converter

Dual –Loop PI Controlled DC-DC Boost Converter

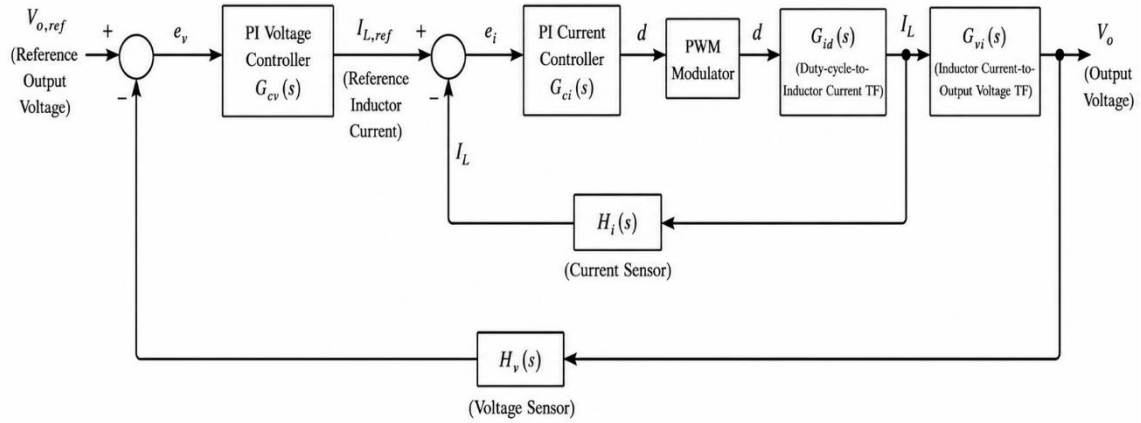

$V_o ref$: Reference output voltage

V_o : Output voltage

$I_{L,ref}$: Inductor current reference

e_i : Current error

I_L :Inductor current

d :Duty cycle ($0<d<1$)

e_v :Voltage error

$G_{vi}(s)$:PI Controller of current loop

$H_v(s)$: Voltage sensor transfer function

$H_i(s)$:Current sensor transfer function

PWM :Pulse width modulator

5.2 Simulation result

Here the simulation result of Dual Loop Boost Converter is shown below .

Fig 5.2 Output voltage waveform of the Boost Converter and Fig5.3 Input inductor current Waveform.

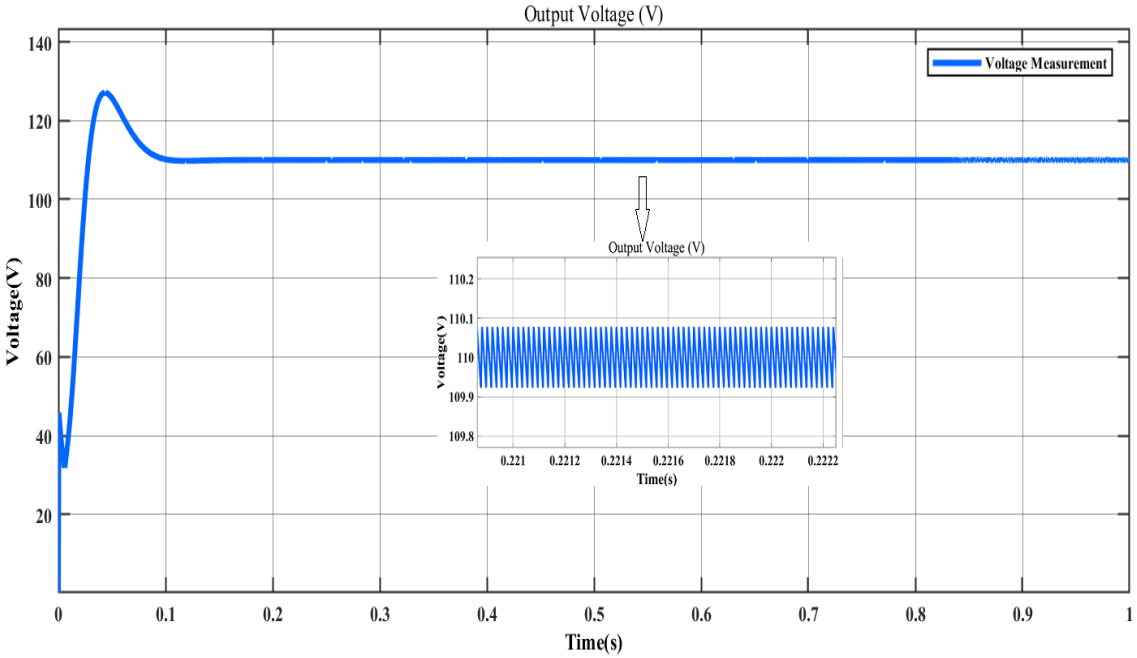

Fig 5.2: Output voltage waveform of Boost Converter

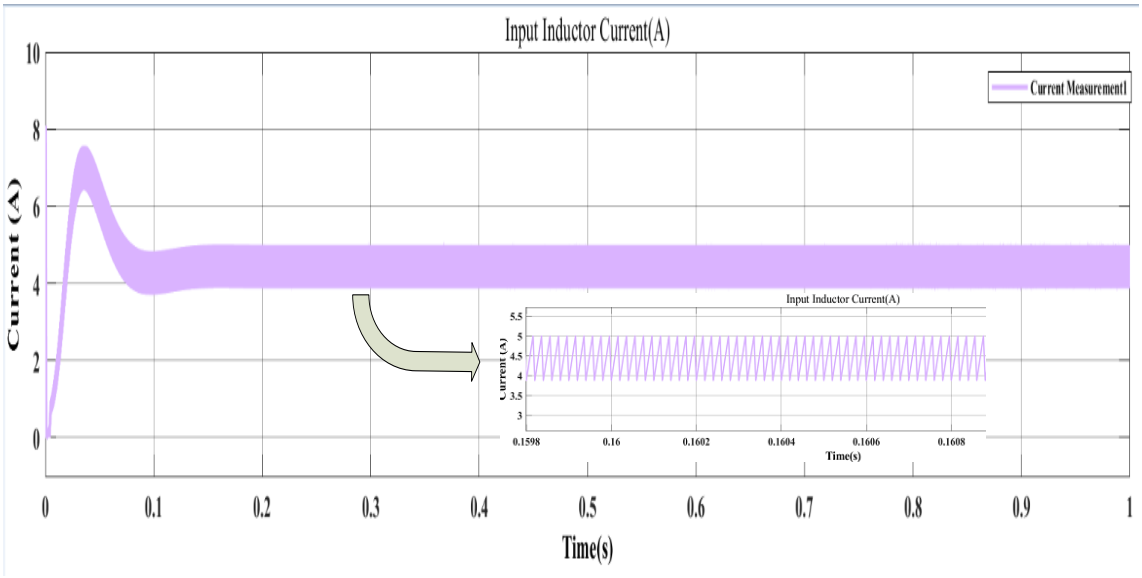

Fig 5.3: Input inductor current waveform of Boost Converter

The output voltage response of the boost converter demonstrates effective voltage regulation and stable converter performance. At the beginning of the operation, the output voltage increases rapidly and shows a slight overshoot before reaching the desired reference value of approximately 110 V. After the transient period, the waveform settles quickly and maintains a constant voltage with very small fluctuations. The smooth steady-state response indicates that the PI-controlled boost converter achieves fast settling time, good stability, and satisfactory dynamic performance. The inductor current waveform shows a rapid rise during startup with a small overshoot before settling at approximately 4.5 A. Once the transient, the current is stable and the ripple is quite small, which shows the stability of the operation of the PI-controlled boost converter and good current regulation. The Bode plot of the current control loop is the frequency response behavior of the boost converter system. The response in magnitude is decreasing with increasing frequency, indicating suppression of high-frequency disturbances and switching noise. The higher the gain at lower frequencies, the more accurate the tracking performance and the more proper the current regulation will be. The phase response is smooth throughout the frequency range and this implies stable dynamic response of the control loop. No abrupt phase changes and resonant peaks indicate a stable converter operation without oscillation.

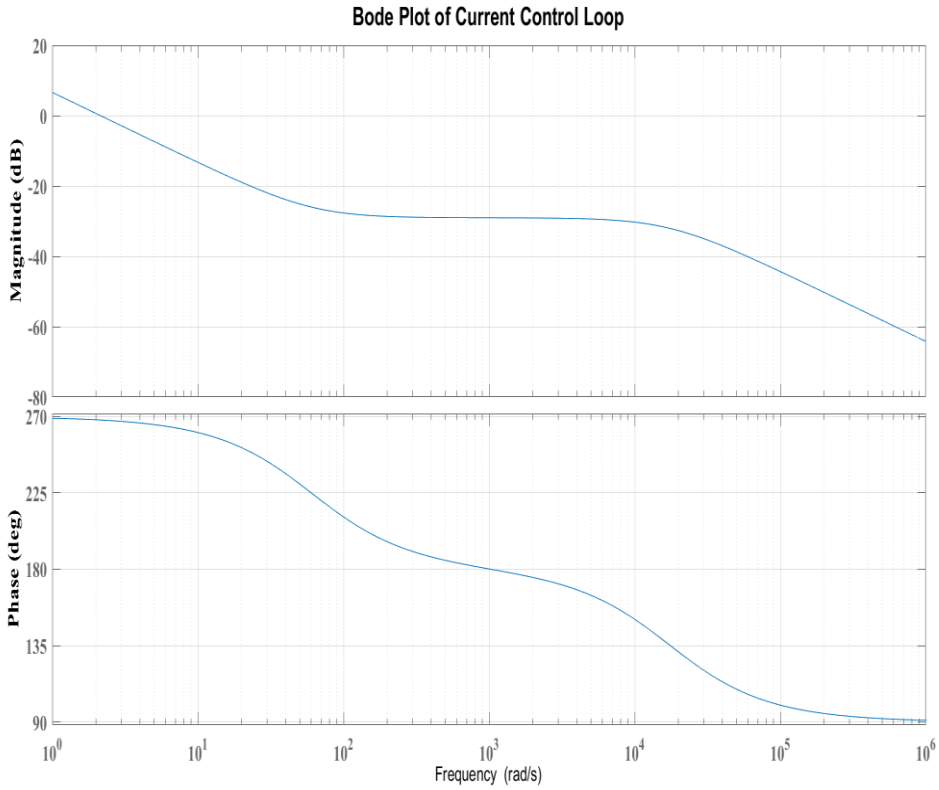

Fig 5.6: Bode Plot for $\hat{i}_L(s)/\hat{d}(s)$

Overall, the frequency response analysis demonstrates that the designed current control loop provides stable operation, good dynamic performance, and effective disturbance rejection for the boost converter system. For the current-controlled boost converter, the root locus plot displays the movement of closed-loop poles as the controller gain varies. Stable system operation is shown by the poles' continued presence in the left side of the complex plane.

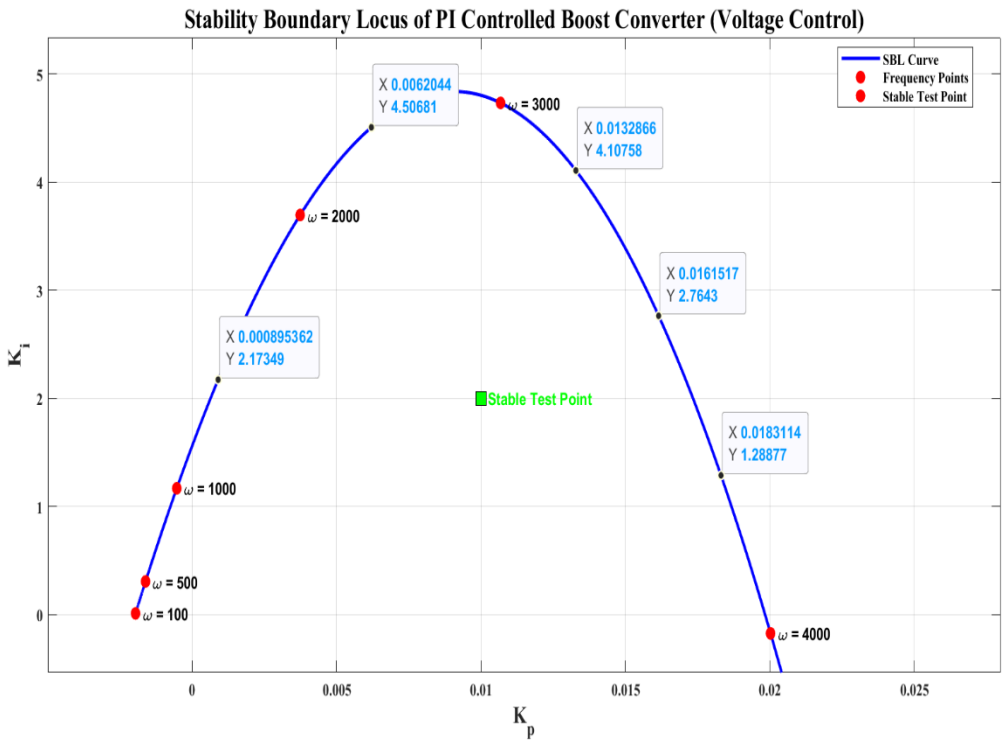

Fig 5.8: SBL of PI Controlled Boost Converter for Voltage control

The figure shows the Stability Boundary Locus (SBL) of the PI-controlled boost converter for voltage control operation. The plot represents the relationship between the proportional gain (Kp) and integral gain (Ki) at different angular frequency values (ω) The SBL curve is useful for identifying the stable operating region of the controller parameters. The horizontal axis represents the proportional gain (Kp) whereas the vertical axis represents the integral gain (Ki).

The blue curve indicates the stability boundary generated for different frequency values. Red points on the curve correspond to selected angular frequencies such as ω=100 , 500, 1000, 2000, 3000, and 4000 rad/s. The green square represents the selected stable test point used for controller validation. From the plot, different stabilizing combinations of Kp and Ki are obtained. Some important gain values identified from the curve. The plot indicates that the stable operating region lies within the stability boundary curve. The selected test point (Kp=0.01, Ki=2) is located inside the stable region, confirming stable closed-loop operation of the boost converter.

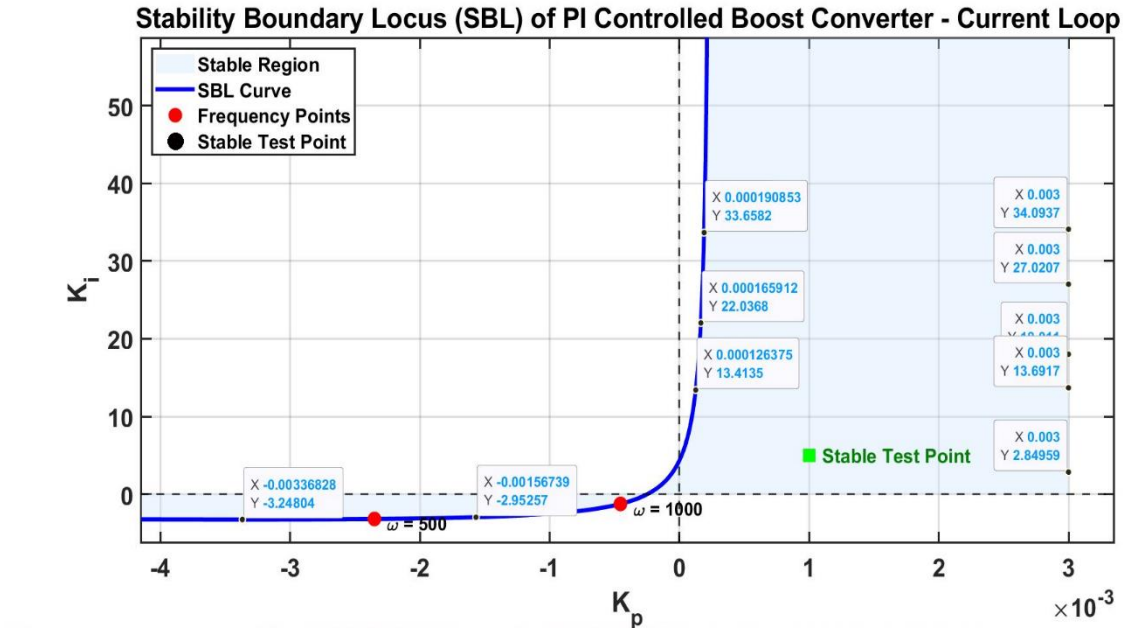

Fig 5.9: SBL of PI Controlled Boost Converter for Current control

The Stability Boundary Locus (SBL) plot for current control shows the stable combinations of proportional gain (Kp) and integral gain (Ki) for the PI-controlled boost converter. The blue curve represents the stability boundary, while the shaded region indicates stable operating conditions. The selected stable test point lies within the stable region, confirming stable current regulation and proper dynamic performance of the converter system.

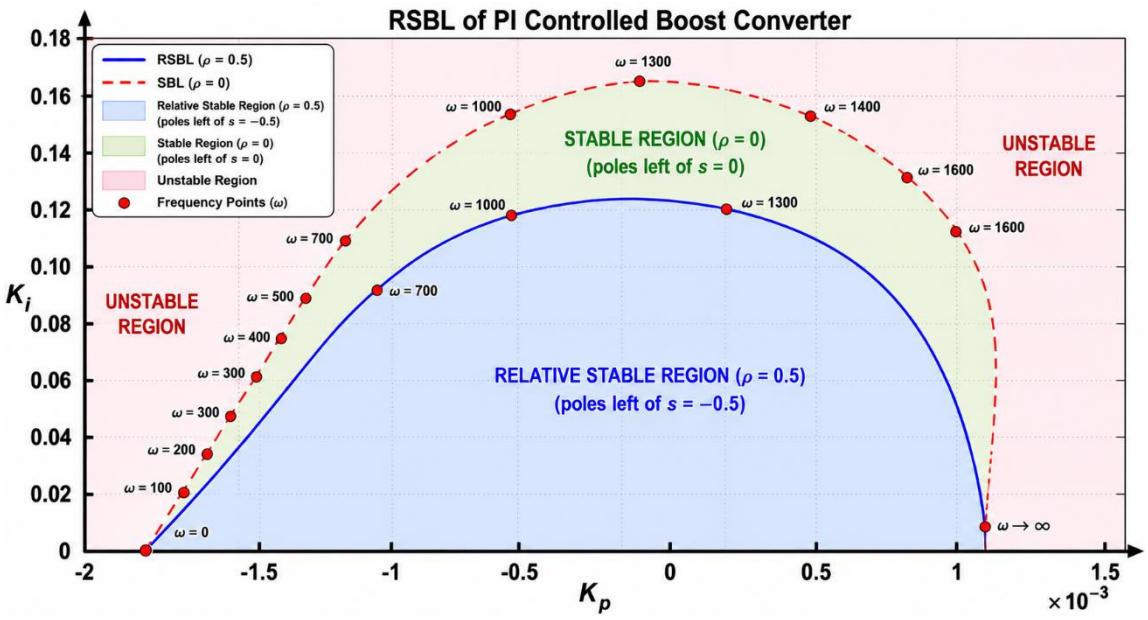

Fig5.10: RSBL of PI Controlled Boost Converter for Voltage control

The figure illustrates the Relative Stability Boundary Locus of the PI-controlled boost converter. The plot shows the variation of proportional gain (Kp) and integral gain (Ki)for different angular frequency values (ω) under relative stability conditions. The horizontal axis represents Kp whereas the vertical axis represents Ki.The blue curve indicates the relative stability boundary, and the red points correspond to selected frequency values such as ω=50, 100, 150, 200, 300, 400, and 500rad/s.

The green square represents the selected stable operating point used for controller analysis. From the plot, it can be observed that the integral gain decreases gradually with increase in proportional gain. The selected stable point lies within the stable region, confirming stable closed-loop operation of the boost converter. The smooth nature of the boundary curve indicates consistent controller behavior and proper tuning characteristics. The selected controller gains provide improved damping, reduced oscillations, and satisfactory transient response of the system. Hence, the Relative Stability Boundary Locus method provides a useful approach for selecting suitable PI controller gains to achieve stable and reliable operation of the boost converter.

CHAPTER 6

CONCLUSION AND FUTURE WORK

6.1 Conclusion

The problem of deriving the whole range of stabilizing parameters of the PI and PID controllers for linear time-invariant systems is solved in this work by using the Stability Boundary Locus (SBL) technique. The method has been developed as a direct and systematic graphical procedure to find a stable region in the Kp and Ki parameter plane, unlike the traditional tuning methods, which rely on repeated tuning, trial and error or optimization procedures. The stability boundaries were obtained by separating the real and imaginary parts of the closed loop characteristic equation, which enabled easy identification of the stable and unstable operating regions**.**

6.2 Future Prospects

This study shown that the Stability Boundary Locus approach may be applied to a variety of systems for controller design, including models for boost converters, unstable systems, and non-minimum phase system. The simulation results showed that the controllers obtained from boundary locus plots are stable and reliable closed-loop controllers. The method was also extended to meet the gain, phase and relative stability requirements using pole shifting techniques. Moreover, interval analysis based on Kharitonov technique was applied to uncertain systems analysis and to guarantee robust stability. In summary, the suggested technique provides a simple, efficient and reliable method for the design of PI/PID controllers in different engineering applications.

REFERENCES

[1] R. W. Erickson and D. Maksimović, *Fundamentals of Power Electronics*, 2nd ed. New York, USA: Springer, 2001.

[2] N. Mohan, T. M. Undeland, and W. P. Robbins, *Power Electronics: Converters, Applications and Design*, 3rd ed. Hoboken, NJ, USA: Wiley, 2003.

[3] K. J. Åström and T. Hägglund, *PID Controllers: Theory, Design, and Tuning*, 2nd ed. Research Triangle Park, NC, USA: ISA, 1995.

[4] M. H. Rashid, *Power Electronics: Circuits, Devices and Applications*, 4th ed. Noida, India: Pearson Education, 2014.

[5] N. Tan, I. Kaya, C. Yeroglu, and D. P. Atherton, "Computation of stabilizing PI and PID controllers using the stability boundary locus," *Energy Conversion and Management*, vol. 47, no. 18–19, pp. 3045–3058, Nov. 2006.

[6] J. C. Ziegler and N. B. Nichols, "Optimum settings for automatic controllers," *Transactions of the ASME*, vol. 64, pp. 759–768, 1942.

[7] K. J. Åström, T. Hägglund, C. C. Hang, and W. K. Ho, "Automatic tuning and adaptation for PID controllers—A survey," *Control Engineering Practice*, vol. 1, no. 4, pp. 699–714, 1993.

[8] K. J. Åström and T. Hägglund, *PID Controllers: Theory, Design, and Tuning*. Research Triangle Park, NC, USA: Instrument Society of America, 1995.

[9] W. K. Ho, C. C. Hang, and L. S. Cao, "Tuning of PID controllers based on gain and phase margin specifications," *Automatica*, vol. 31, no. 3, pp. 497–502, 1995.

[10] M. T. Ho, A. Datta, and S. P. Bhattacharyya, "A linear programming characterization of all stabilizing PID controllers," in *Proceedings of the American Control Conference*, 1997, pp. 3929–3933.

[11] M. T. Söylemez, N. Munro, and H. Baki, "Fast calculation of stabilizing PID controllers," *Automatica*, vol. 39, no. 1, pp. 121–126, 2003.

[12] N. Tan and D. P. Atherton, "Feedback stabilization using the Hermite–Biehler theorem," in *International Conference on the Control of Industrial Processes*, Newcastle, U.K., 1999.

[13] J. Ackermann and D. Kaesbauer, “Design of robust PID controllers,” in *European Control Conference*, 2001, pp. 522–527.

[14] Z. Shafei and A. T. Shenton, “Frequency domain design of PID controllers for stable and unstable systems with time delay,” *Automatica*, vol. 33, no. 12, pp. 2223–2232, 1997.

[15] N. Mohan, T. Undeland, and W. Robbins, *Power Electronics: Converters, Applications and Design*, Wiley, 2003.

[16] R. W. Erickson and D. Maksimovic, *Fundamentals of Power Electronics*, Springer, 2001.

[17] K. Ogata, *Modern Control Engineering*, Prentice Hall, 2010.

[18] A. Datta, M. T. Ho, and S. P. Bhattacharyya, *Structure and Synthesis of PID Controllers*, Springer, 2000.

[19] S. P. Bhattacharyya, H. Chapellat, and L. H. Keel, *Robust Control: The Parametric Approach*, Prentice Hall, 1995.

[20] M. Veerachary, “Power Tracking for Nonlinear PV Sources With Coupled Inductor SEPIC Converter,” *IEEE Transactions on Aerospace and Electronic Systems*, vol. 41, no. 3, pp. 1019–1029, July 2005.

[21] T. Bajd, M. Rodič, and I. Škrjanc, *Design of Stabilizing PID Controllers Using Stability Boundary Locus Method*, Springer, 2018.

[22] Power Electronics: Circuits, Devices and Applications, 4th ed., Pearson Education, 2014.

[23] K. Ogata, *Modern Control Engineering*, 5th ed., Prentice Hall, 2010.

[24] J. G. Ziegler and N. B. Nichols, “Optimum settings for automatic controllers,” *Transactions of the ASME*, vol. 64, no. 11, pp. 759–768, 1942.

[25] Fundamentals of Power Electronics, Springer, 2001.

[26] R. W. Erickson, “DC–DC power converters,” *Wiley Encyclopedia of Electrical and Electronics Engineering*, Wiley, 1999.

[27] Y. Shi and R. Eberhart, “A modified particle swarm optimizer,” *IEEE International Conference on Evolutionary Computation*, pp. 69–73, 1998.

[28] N. Tan, I. Kaya, C. Yeroglu, and D. P. Atherton, “Computation of stabilizing PI and PID controllers using the stability boundary locus,” *Energy Conversion and Management*, vol. 47, no. 18–19, pp. 3045–3058, 2006.

[29] G. J. Silva, A. Datta, and S. P. Bhattacharyya, *PID Controllers for Time-Delay Systems*, Birkhäuser, 2005.

[30] M. Debbat, A. Bousselham, and M. Belazzoug, "PI controller design for DC–DC boost converter using stability region approach," *International Journal of Power Electronics and Drive Systems*, vol. 9, no. 2, pp. 761–770, 2018.

[31] M. T. Ho, A. Datta, and S. P. Bhattacharyya, *Structure and Synthesis of PID Controllers*, Springer, London, 2000.

[32] S. Choudhary and D. K. Palwalia, "Performance analysis of PI and PID controllers for DC–DC boost converter," *International Journal of Engineering Research and Applications*, vol. 4, no. 7, pp. 117–123, 2014.

[33] A. Elkhateb, N. Abd Rahim, J. Selvaraj, and B. W. Williams, "Fuzzy-logic-controller-based SEPIC converter for maximum power point tracking," *IEEE Transactions on Industry Applications*, vol. 50, no. 4, pp. 2349–2358, 2014.